PRODUCTION CROSS SECTIONS OF $e^{\pm}$ AND γ RAYS

Luca Orusa

XSCRC2024: Cross sections for Cosmic Rays

CERN, 17/10/2024

Luca Orusa, Mattia Di Mauro, Fiorenza Donato, Michael Korsmeier

arXiv:2203.13143, Phys. Rev. D 105 (2022), 123021

arXiv:2302.01943, Phys. Rev. D 107 (2023), 083031

https://github.com/lucaorusa/

PRINCETON UNIVERSITY

COLUMBIA UNIVERSITY IN THE CITY OF NEW YORK

The positron excess (Orusa et al. 2024 arXiv:2410.10951)

- AMS-02 e^+ flux measurements → secondary + primary contribution.

- Pulsars as sources of cosmic-ray $e^{\pm}$.

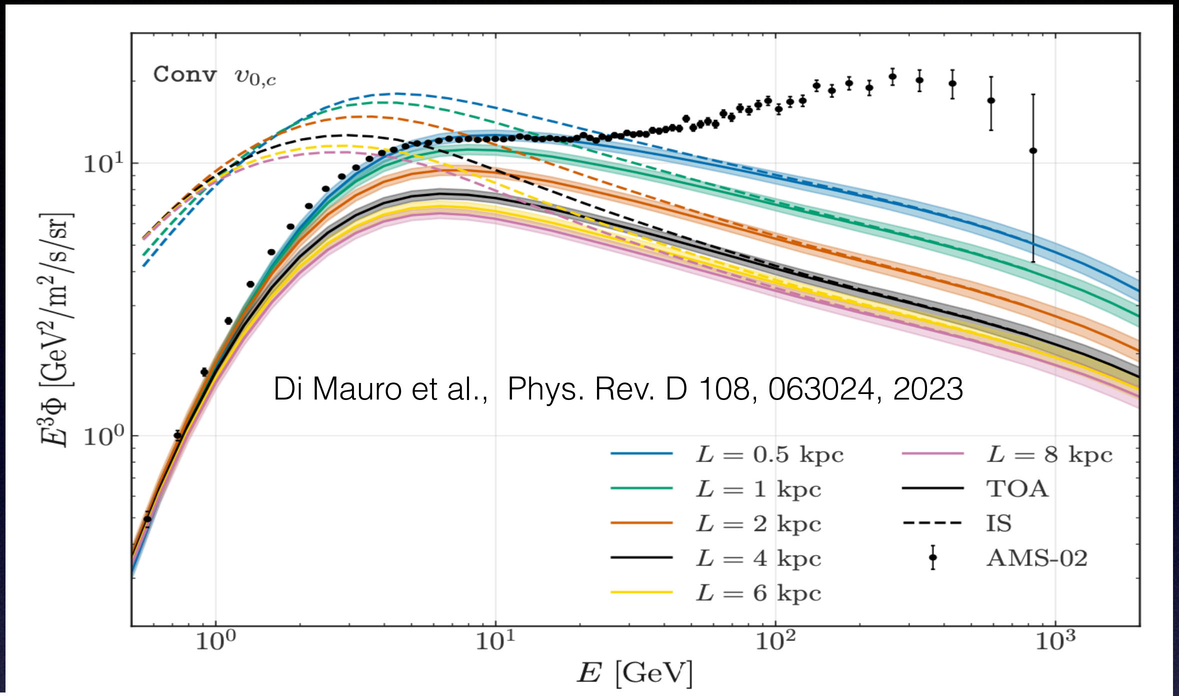

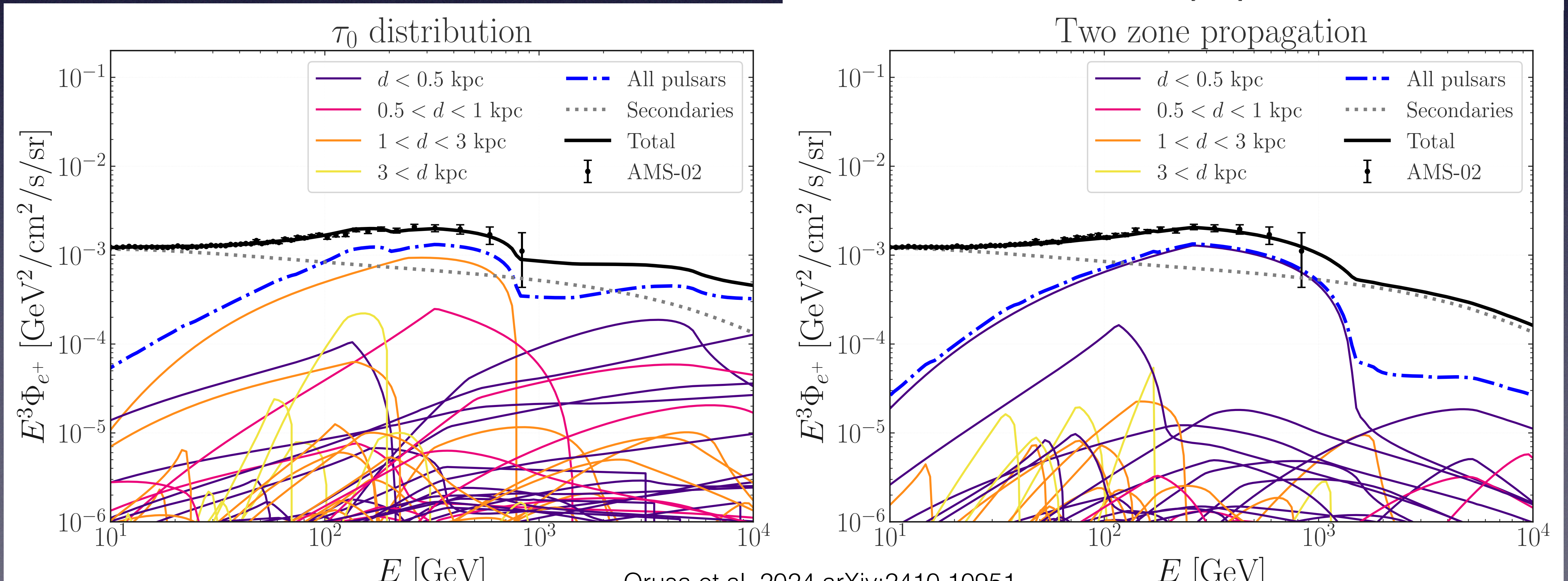

Orusa et al. 2024 arXiv:2410.10951

Secondary positrons

- Secondary contribution:

$$q(T_{e^+}) = \sum_{i,j} 4\pi\, n_{\mathrm{ISM},j} \times$$

$$\int dT_i\, \phi_i(T_i) \frac{d\sigma_{ij}}{dT_{e^+}}(T_i, T_{e^+})$$

- Scattering of a relativistic cosmic ray nucleus i colliding with an interstellar nucleus j at rest:

$$\sigma_{\mathrm{inv}}^{(ij)} = E_{\pi^\pm} \frac{d^3\sigma_{ij}}{dp^3_{\pi^\pm}}(\sqrt{s}, p_T, x_R)$$

- $d\sigma(p + H \rightarrow e^\pm + X)$ former predictions affected by a factor 2 of uncertainty.

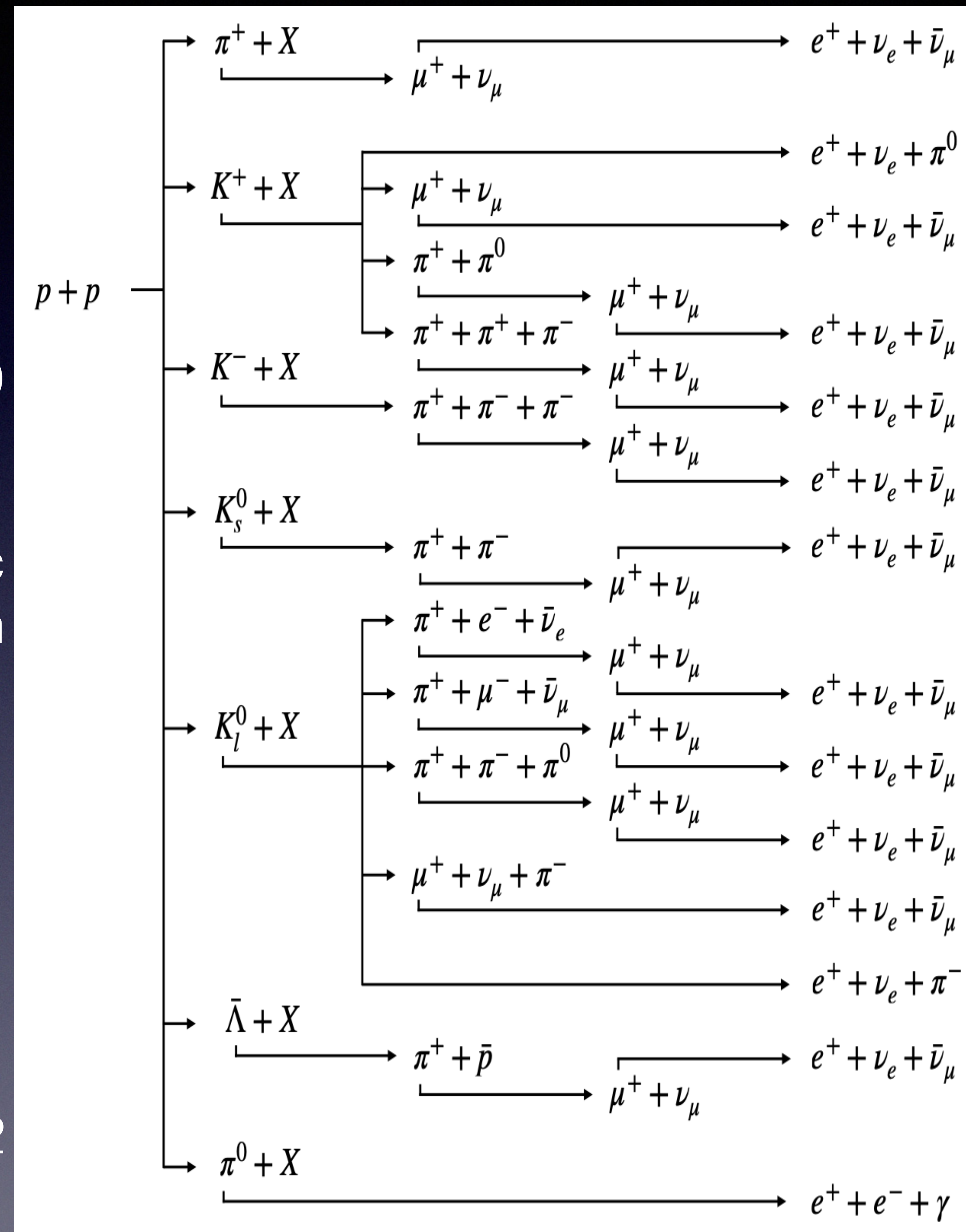

Fit to π^+ data

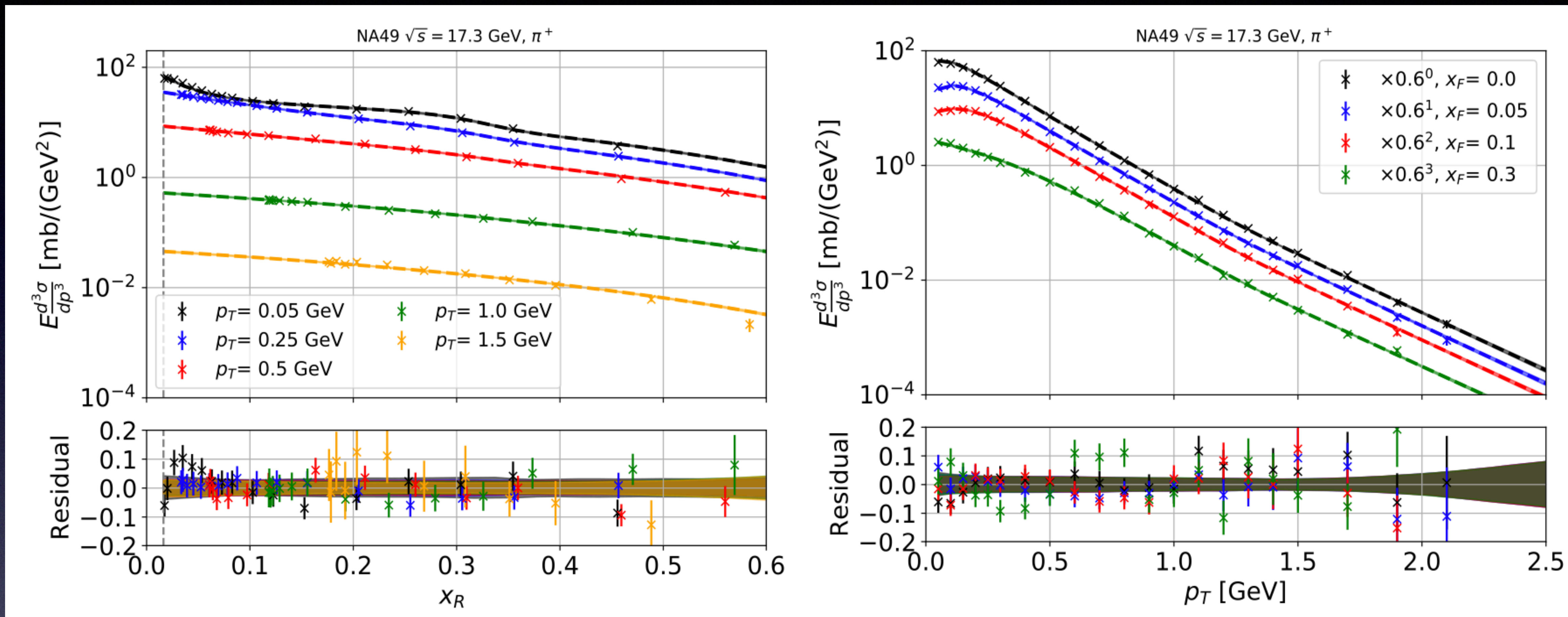

- Total uncertainties between 5 and 10%. $\sqrt{s}$ = 5-50 GeV relevant.
- Integrating σ_{inv} over the solid angle and combining the result with the π^+ decay, we obtain the $\frac{d\sigma_{ij}}{dT_{e^+}}(T_i, T_{e^+})$ from π^+.

Experiment	$\sqrt{s}$ [GeV]		$\sigma_{\rm inv}$	n	Ref.
NA49	17.3	$(\pi^\pm, K^\pm)$	√	-	[67, 76]
ALICE	900	$(\pi^+, K^\pm)$	√	-	[77]
CMS	900, 2760, 7000, 13000	$(\pi^\pm, K^\pm)$	√	-	[78, 79]
Antinucci	3.0, 3.5, 4.9, 5.0, 6.1, 6.8	$(\pi^\pm)$	-	√	[80]
	2.8, 3.0,3.2, 5.3, 6.1, 6.8	(K^+)	-	√	[80]
	4.9, 5.0, 6.1, 6.8	(K^-)	-	√	[80]
NA61/SHINE	6.3, 7.7, 8.8, 12.3, 17.3	$(\pi^\pm, K^\pm)$	-	√	[68]

Other channels

We consider the π^+ created from weak decays of strange particles:

- $K^\pm$, K^0_S: fit on available data.
- K^0_L: rescaled contribution from K^0_S.
- $\bar{\Lambda}, \Sigma$ and Ξ: rescaled contribution from the Λ.

We also consider the contribution from π^0 to the e^+ yield by multiplying the π^+ cross sections by a normalization factor connected to the multiplicity of π^+, π^0.

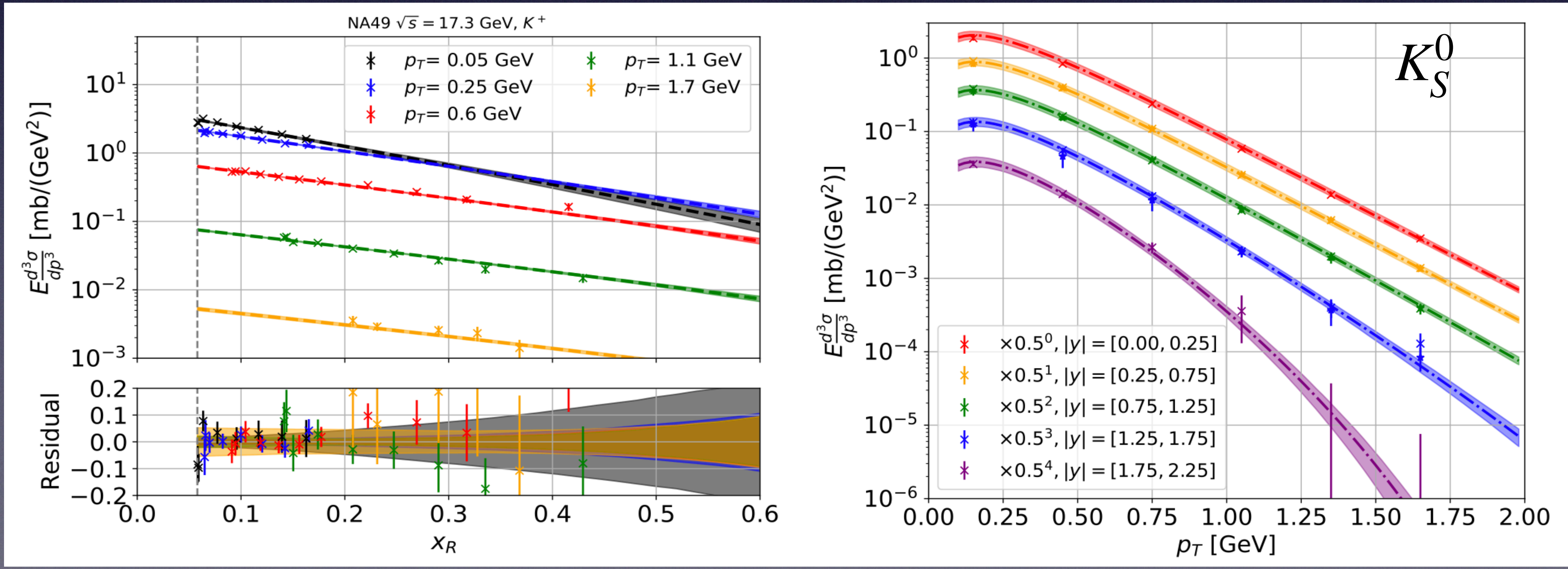

Results on the e^+ production cross section

- The π^+ channel dominates the total cross section (10 times higher than the K^+ channel).
- e^+ production from K^0_S, K^0_L, and subdominant channels contributes at a few % level.
- $d\sigma/dT_{e^+}$ uncertainty: at 1σ is 5% to 8% at all T_p energies.

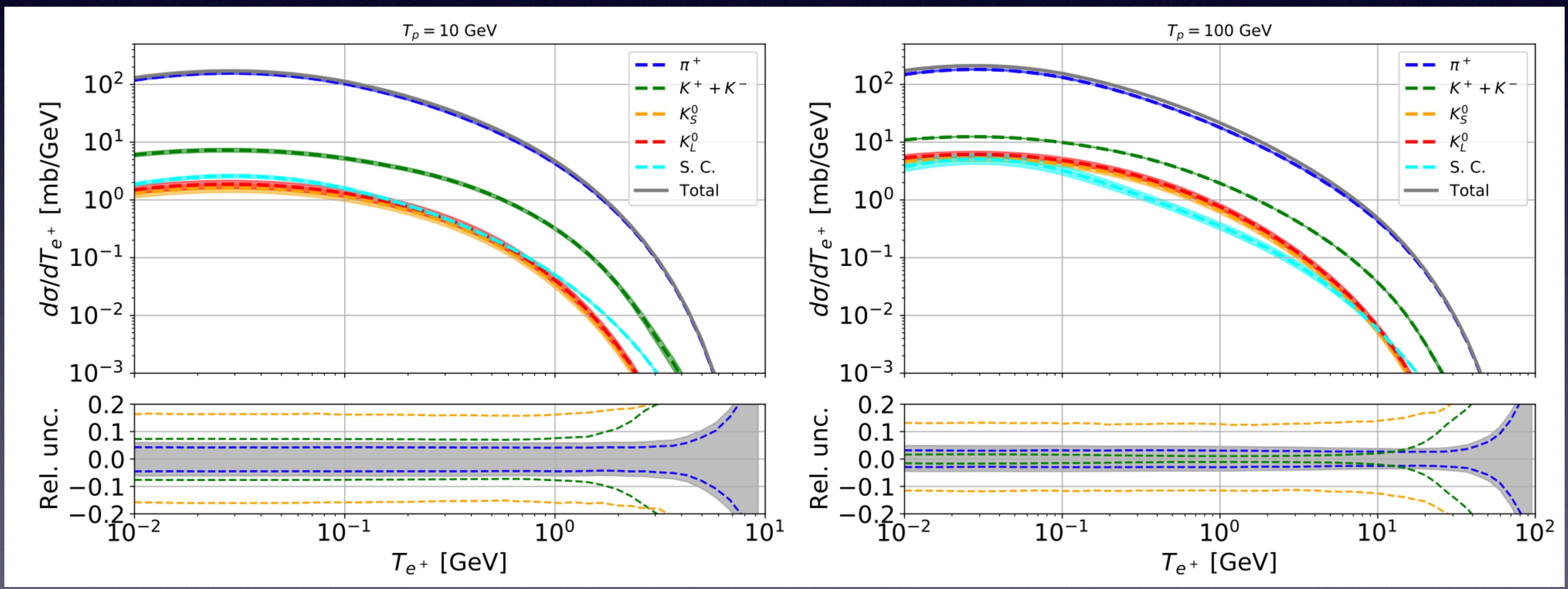

- Secondary e^+ are produced in nuclei interactions ($p + A, A + p$, and $\mathrm{A} + \mathrm{A}$).
- We use data from NA49 for $p + \mathrm{C} \to \pi^+ + \mathrm{X}$ and NA61 for the other channels.

Results on the e^+ production cross section

- The $q(E)$ is predicted with a remarkably small uncertainty, ranging from 5% to 8%.
- The channels involving He, constitute 30-40% of the total spectrum.
- The heavier primary CNO nuclei contribute a non negligible few percent at the AMS-02 energies.

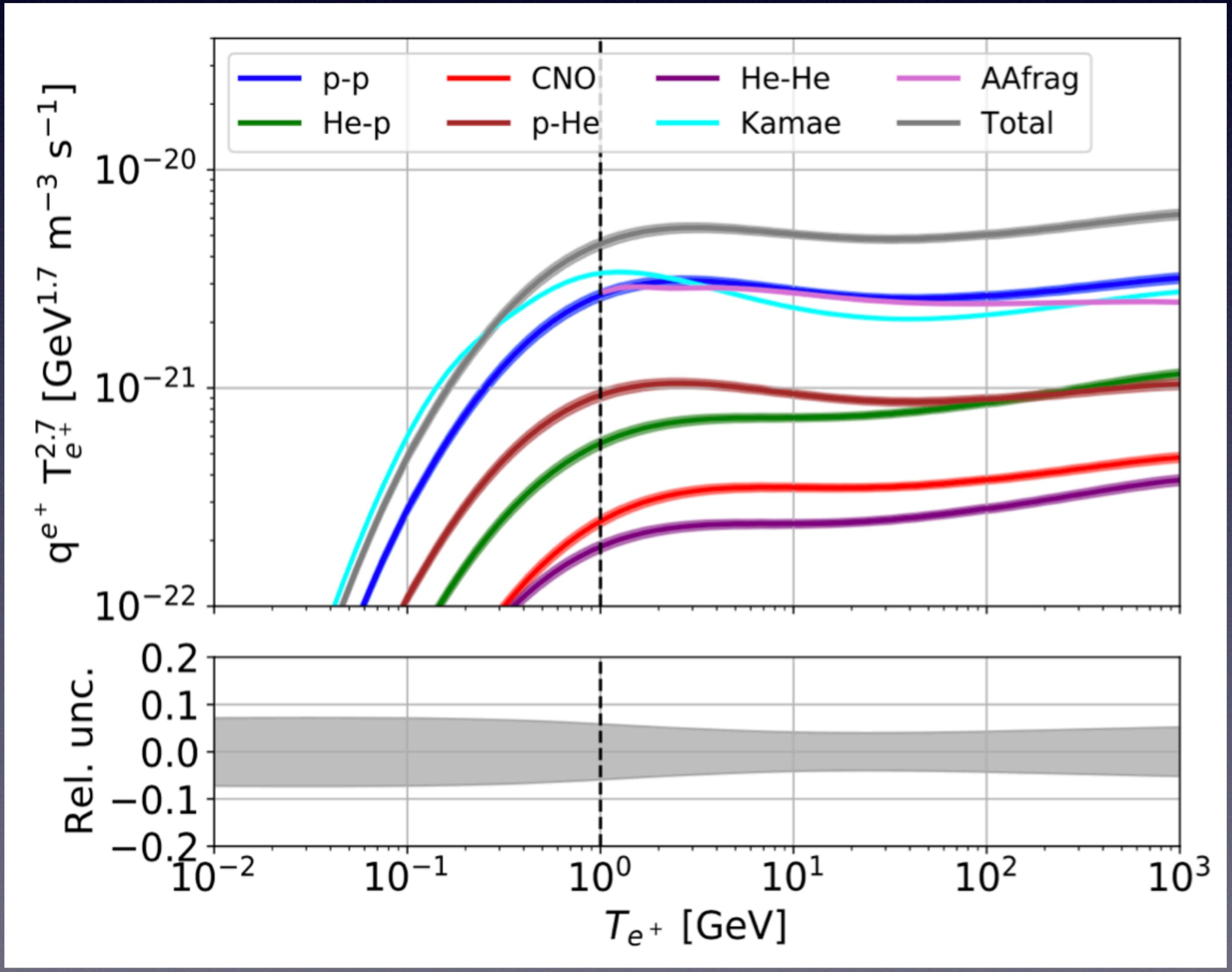

- Similar analysis performed for e^- with similar conclusions.
- Future measurements of pion production in the $p + \mathrm{He}$ could help to improve the predictions for nuclei channels.
- For Monte Carlo predictions, see talk by De la Torre Luque (tomorrow).

Diffuse γ-ray emission

- Most of the γ rays detected by Fermi-LAT are produced by the Galactic diffuse emission.
- It originates from the interaction of CRs with interstellar gas and radiation fields within our own Galaxy.

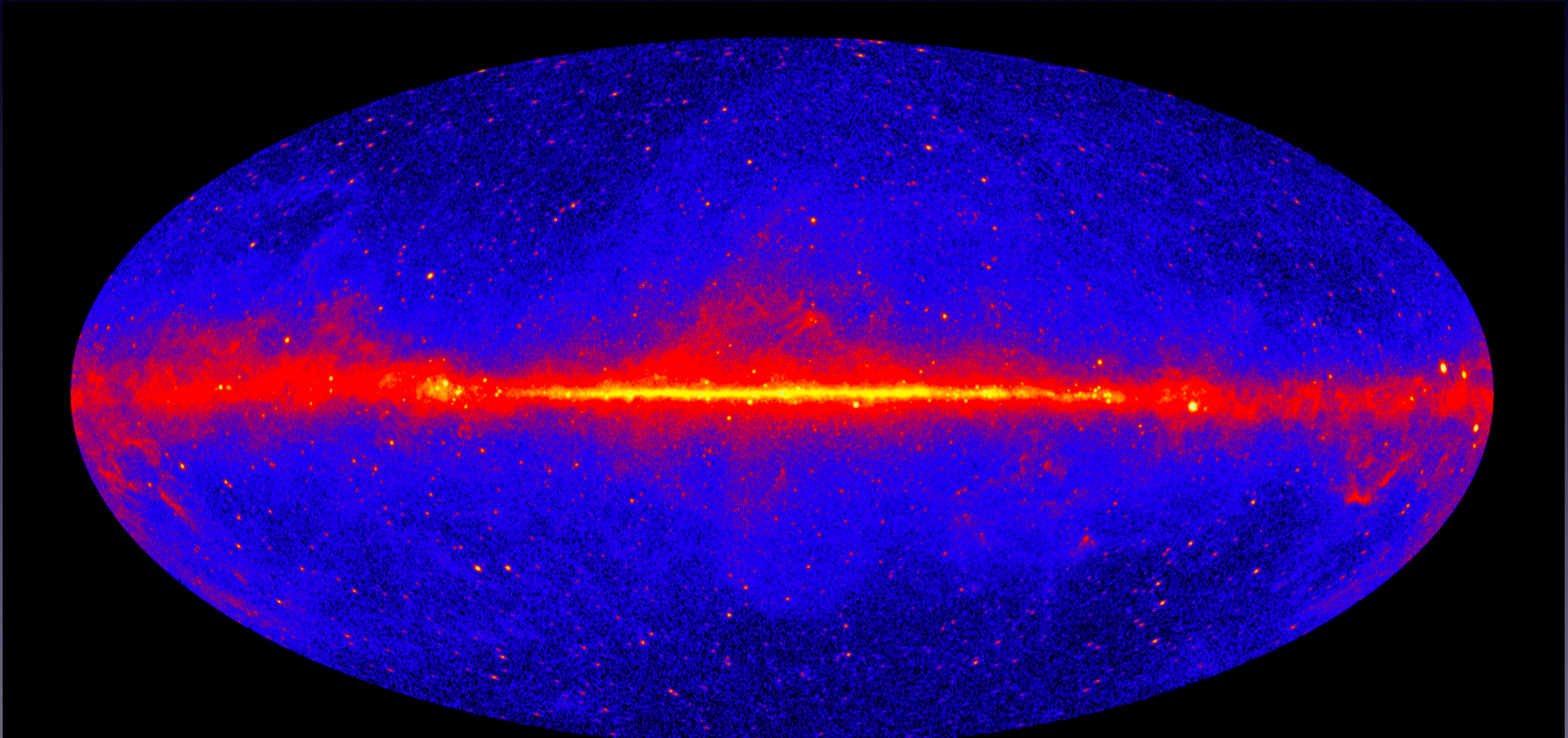

https://svs.gsfc.nasa.gov/14090

- $\sigma(p+p\rightarrow\gamma+X)$: γ-ray production cross section are needed.
- Uncertainties greater than the Fermi-LAT statistical errors undermine the study of the Galactic interstellar emission.
- Galactic Center: a significant excess of γ rays has been observed.

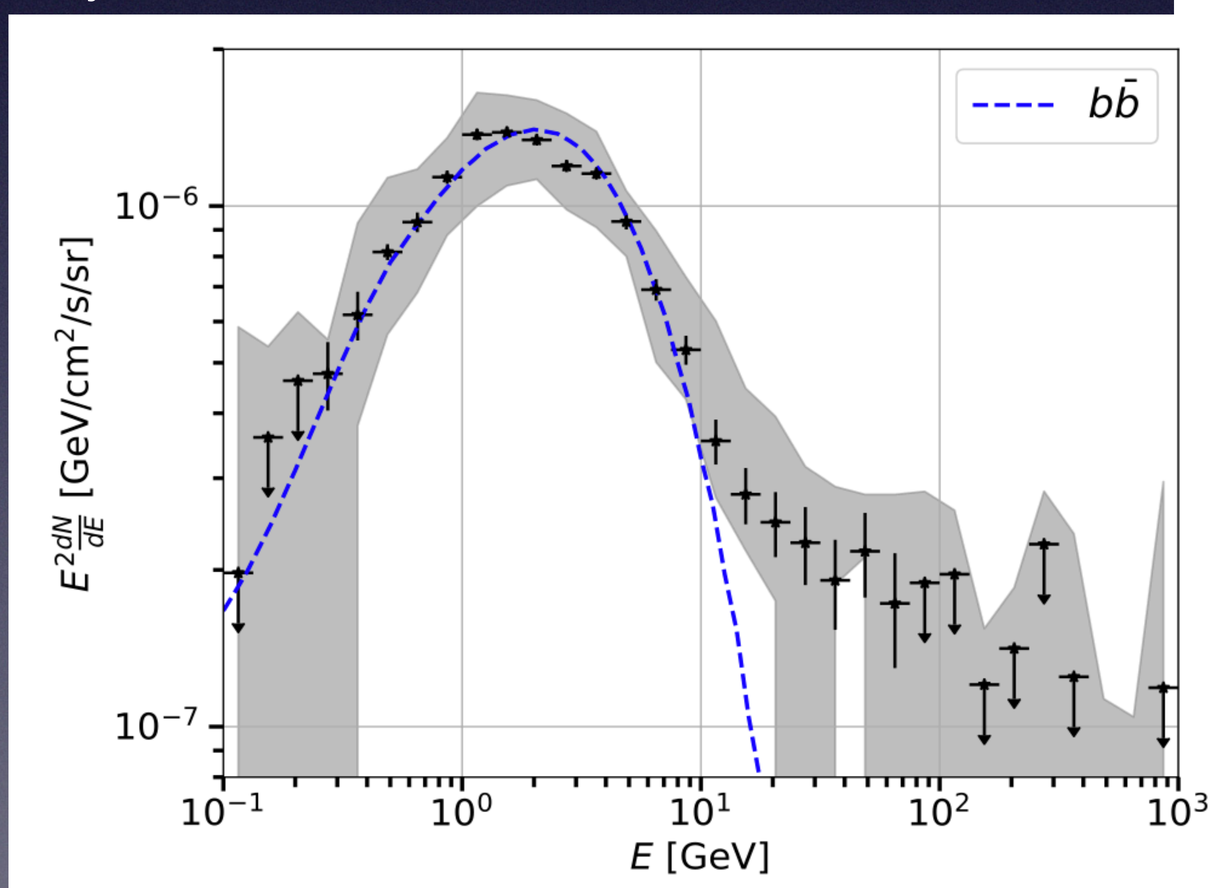

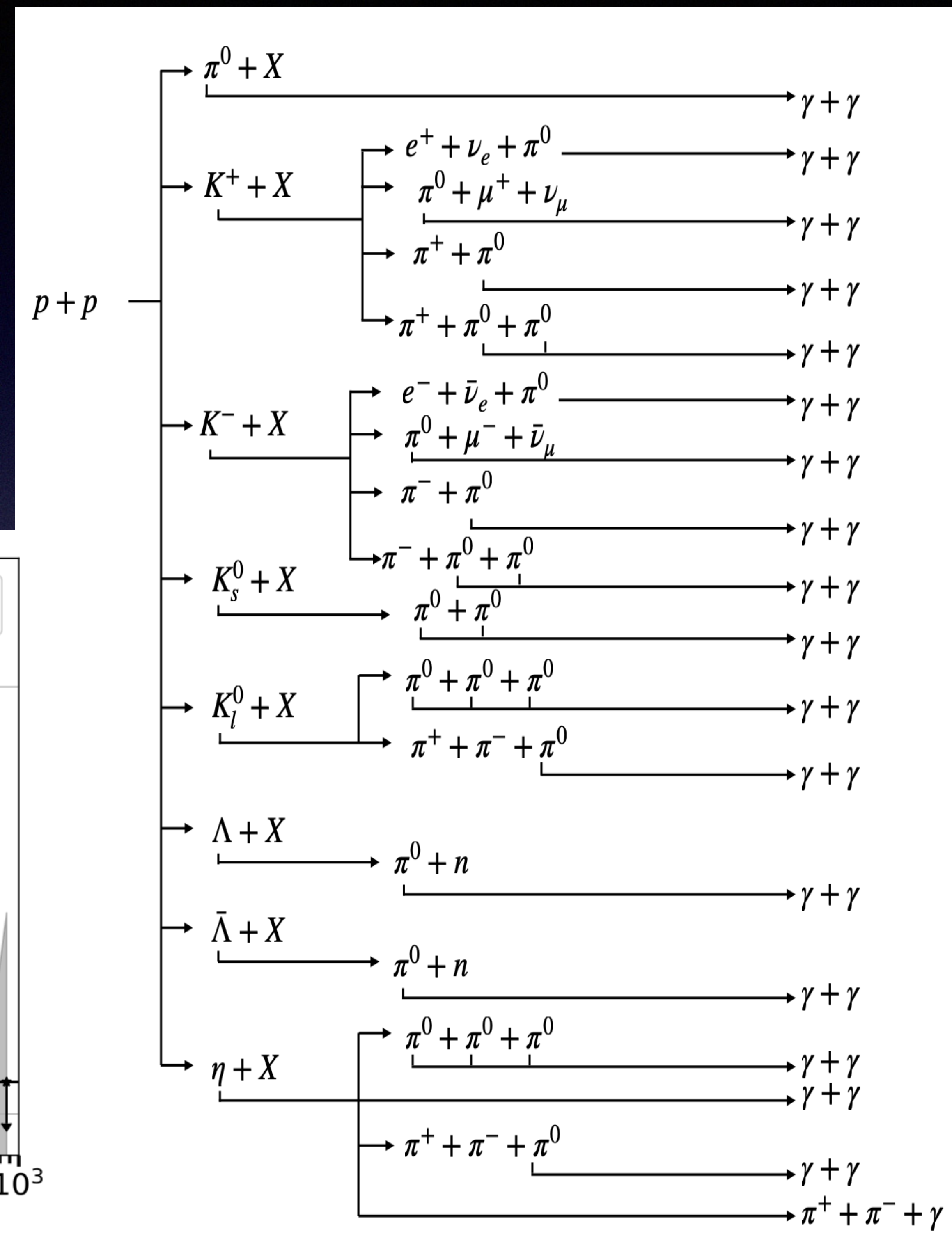

Di Mauro et al., Phys. Rev. D 103, 123005 (2021)

Results on the γ-ray production cross section

$$\sigma_{\text{inv}} = \sigma_0(s)\, c_{20}\, [G_{\pi^+}(p_T, x_R) + G_{\pi^-}(p_T, x_R)]\, A(s)$$

- π^0: total uncertainties between 7 and 20%. $\sqrt{s}$ = 5-50 GeV relevant.
- $K^{\pm}$, K_S^0: fit on available data.
- K_L^0: rescaled contribution from K_S^0.
- η: fit on available data and rescaled contribution from π^0.

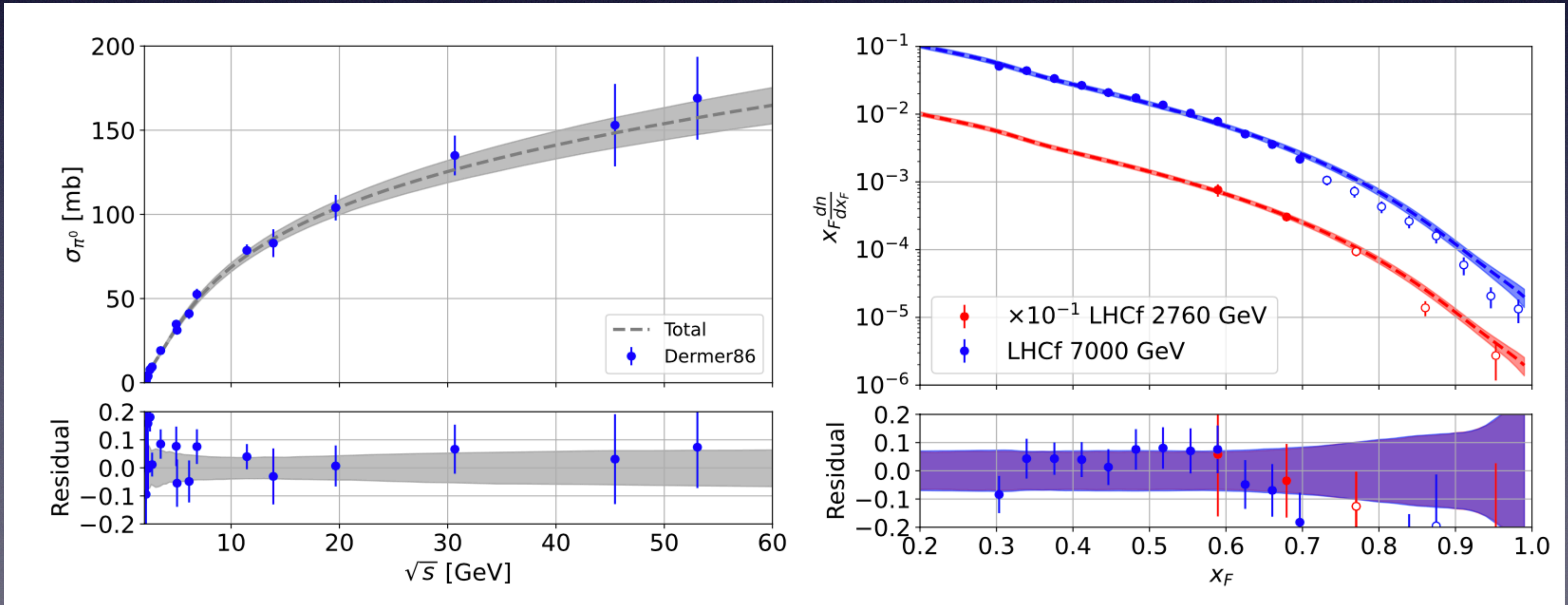

Results on the γ-ray production cross section

- The π^0 channel dominates the total cross section, with final uncertainty from 6% to 20% at different T_p and E_γ (https://github.com/lucaorusa/gamma_cross_section).

- New data from colliders are needed: Lorentz invariant cross section for π^0 productions (p_T < 1 GeV, in $\sqrt{s}$ = 5-50 GeV). Same for He target.

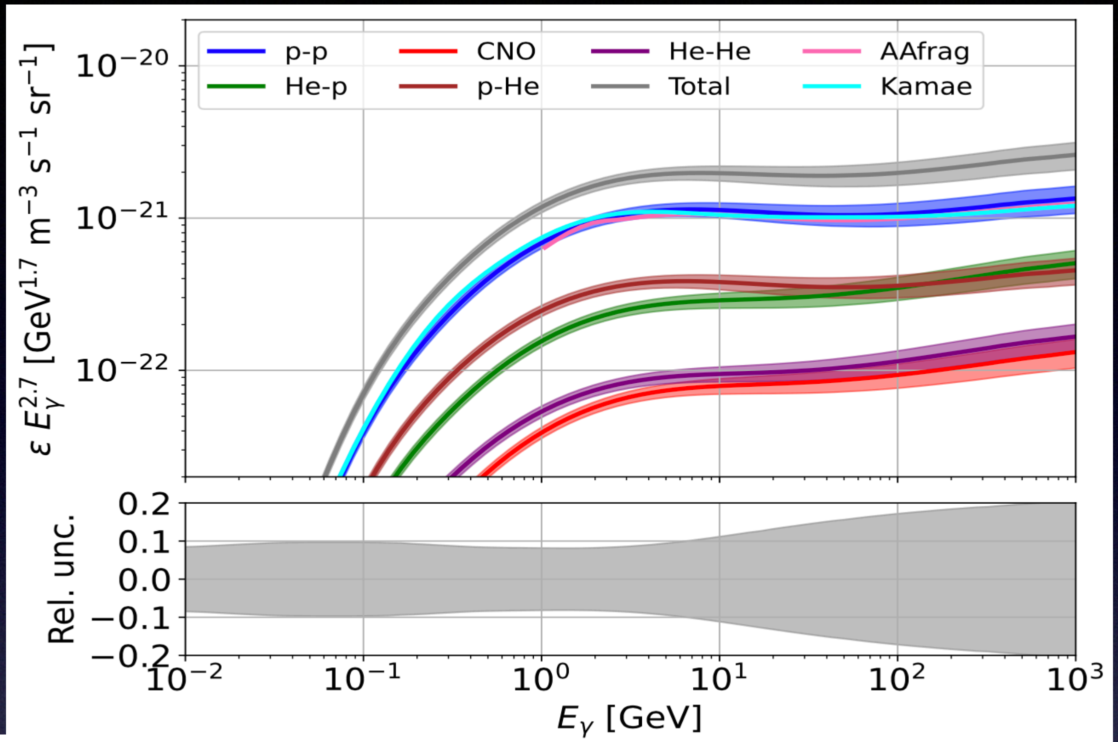

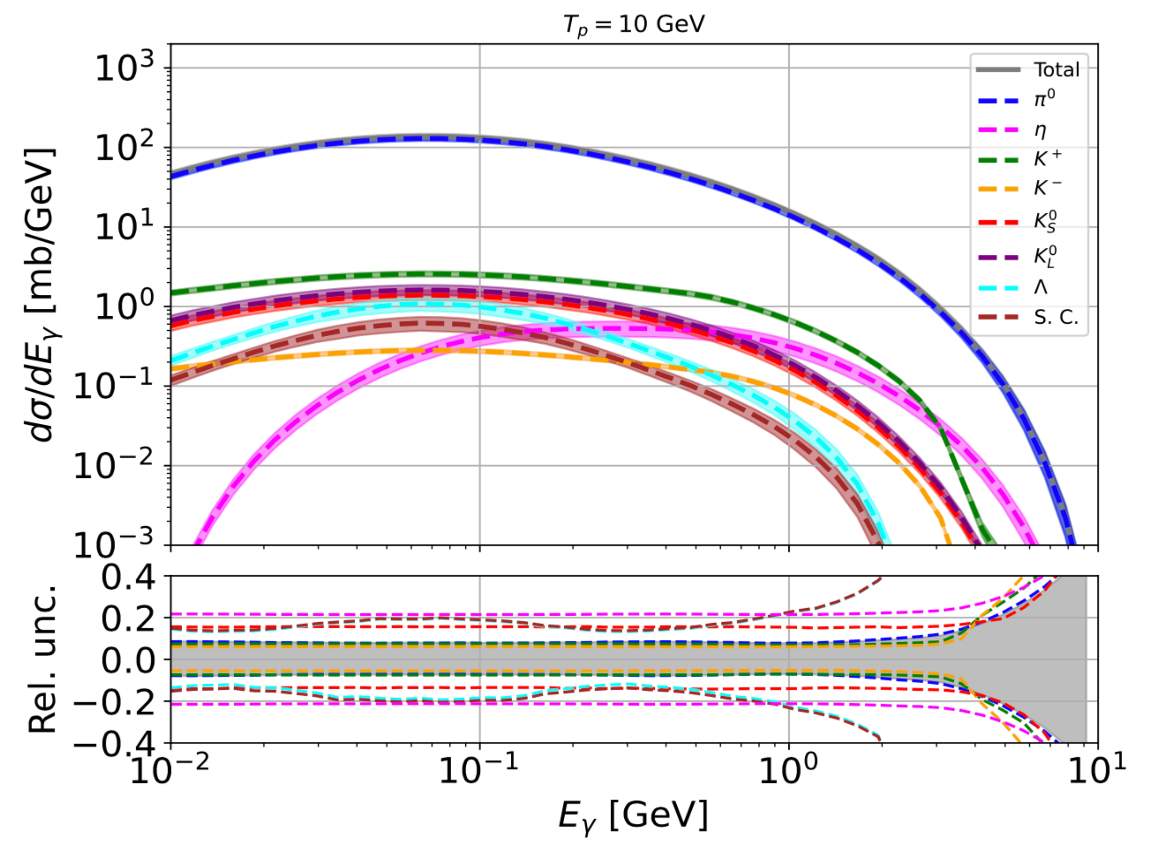

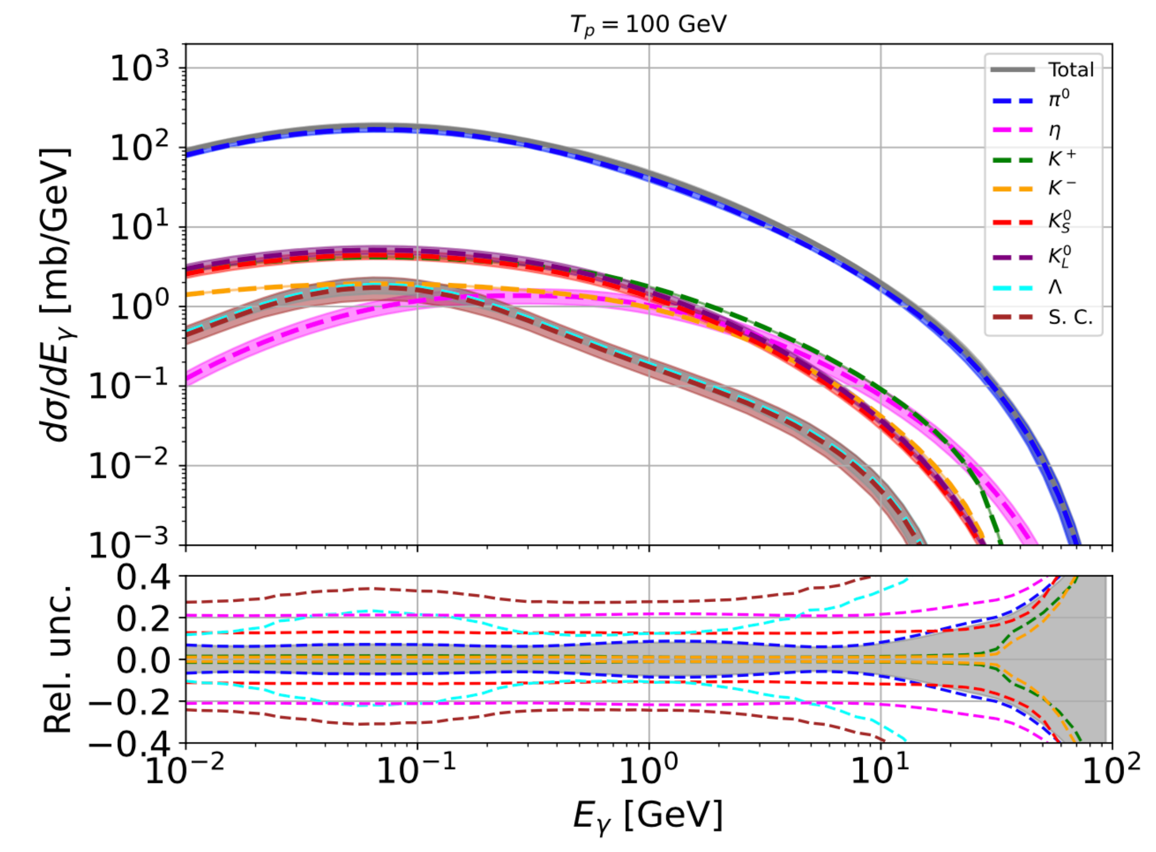

Diffuse ν emission (Orusa et al. in prep)

- Unlike the multi-component fluxes of γ rays, the flux of galactic diffuse ν uniquely originate from the decay of charged mesons, that are produced in hadronic interactions.

- ν production cross section are needed.

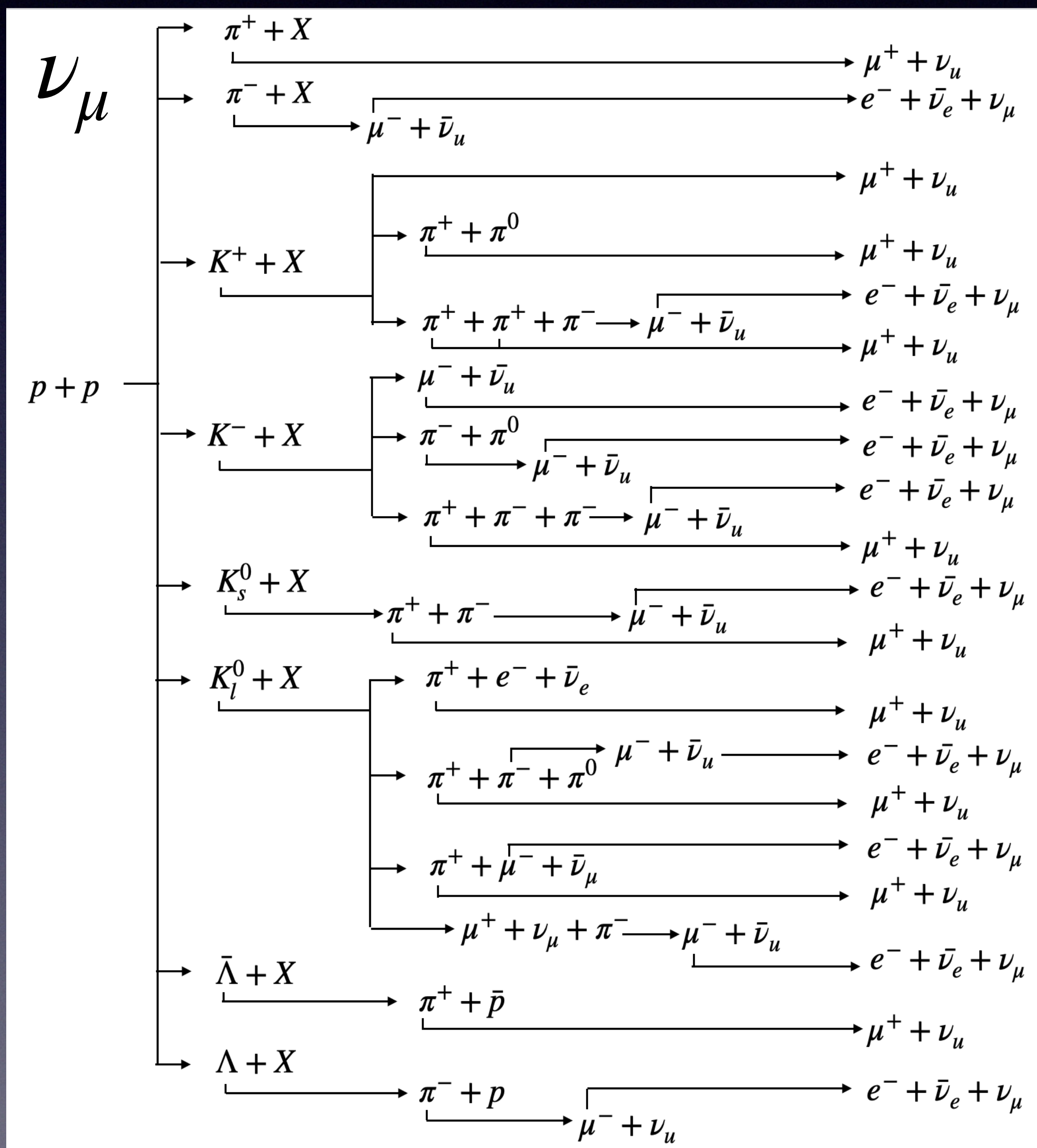

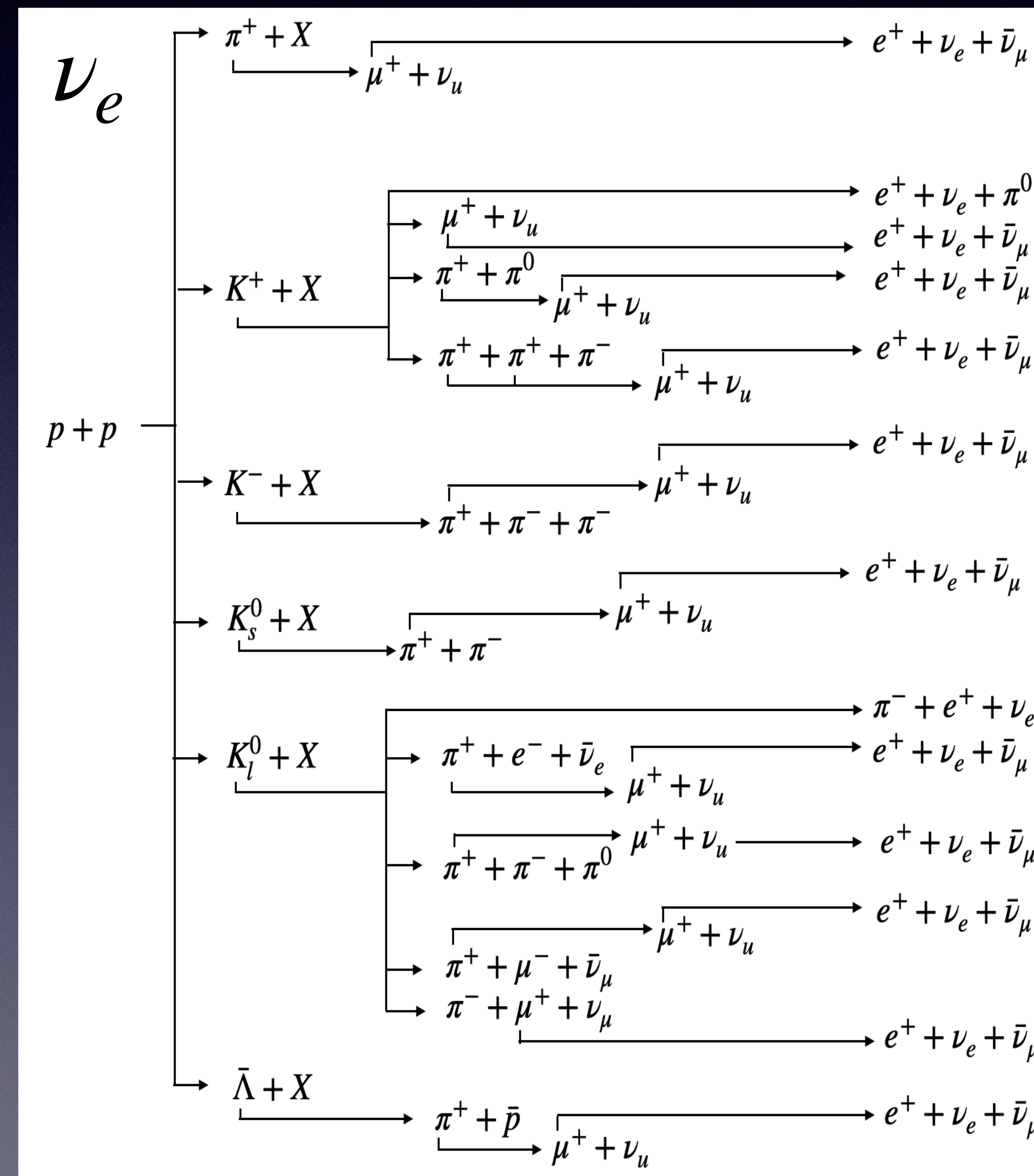

WISH LIST

1. $p + \mathrm{He} \rightarrow e^{+} + X$ ($p + \mathrm{He} \rightarrow \pi^{+} + X$)
   (p beam $\sim 10 - 200$ GeV)

2. $p + p \rightarrow \gamma + X$ ($p + p \rightarrow \pi^{0} + X$)
   (p beam $\sim 10 - 200$ GeV)

3. $p + \mathrm{He} \rightarrow \gamma + X$ ($p + \mathrm{He} \rightarrow \pi^{0} + X$)
   (p beam $\sim 10 - 200$ GeV)

Backup

- $\sigma_{\rm inv} = \sigma_0(s)\, c_1 \left[F_p(s, p_T, x_R) + F_r(p_T, x_R) \right] A(s)$
- $F_p(s, p_T, x_R) = (1 - x_R)^{c_2} \exp(-c_3\, x_R)\, p_T^{c_4} \times \exp\left[-c_5 \sqrt{s/s_0}^{\,c_6} \left(\sqrt{p_T^2 + m_\pi^2} - m_\pi \right)^{c_7 \sqrt{s/s_0}^{\,c_6}} \right]$
- $F_r(p_T, x_R) = (1 - x_R)^{c_8} \times \exp\left[-c_9\, p_T - \left(\frac{|p_T - c_{10}|}{c_{11}} \right)^{c_{12}} \right] \times \left[c_{13} \exp(-c_{14}\, p_T^{c_{15}} x_R) + c_{16} \exp\left(-\left(\frac{|x_R - c_{17}|}{c_{18}} \right)^{c_{19}} \right) \right]$
- $A(s) = \frac{1 + \left(\sqrt{s/c_{20}} \right)^{c_{21} - c_{22}}}{1 + \left(\sqrt{s_0/c_{20}} \right)^{c_{21} - c_{22}}} \left(\sqrt{\frac{s}{s_0}} \right)^{c_{22}}$

	π^+	π^-	K^+	K^-
$\chi^2_{\rm NA49}$/d.o.f.	338/263	287/290.	146/151	197/151
χ^2_{n}/d.o.f.	189/129	169/96	160/102	135/100
$\chi^2_{\rm ALICE}$	77 (33)	-	42 (27)	36 (27)
$\chi^2_{\rm CMS}$	100 (88)	154 (88)	77 (68)	54 (68)
$\chi^2_{\rm NA61, Antinucci}$	10 (12)	15 (12)	39 (11)	44 (9)
$\chi^2_{\rm tot}$/d.o.f.	527/392	456/386	306/253	332/251

Backup

- The uncertainties are about 5% for almost all T_{e^+}.
- The relative uncertainty increases above 20% when approaching the maximum energy, that has a negligible impact on the final uncertainty.
- The results of this Section already hint at the final result. The by far dominant contribution of e^+ production in $p+p$ collisions comes from π^+.

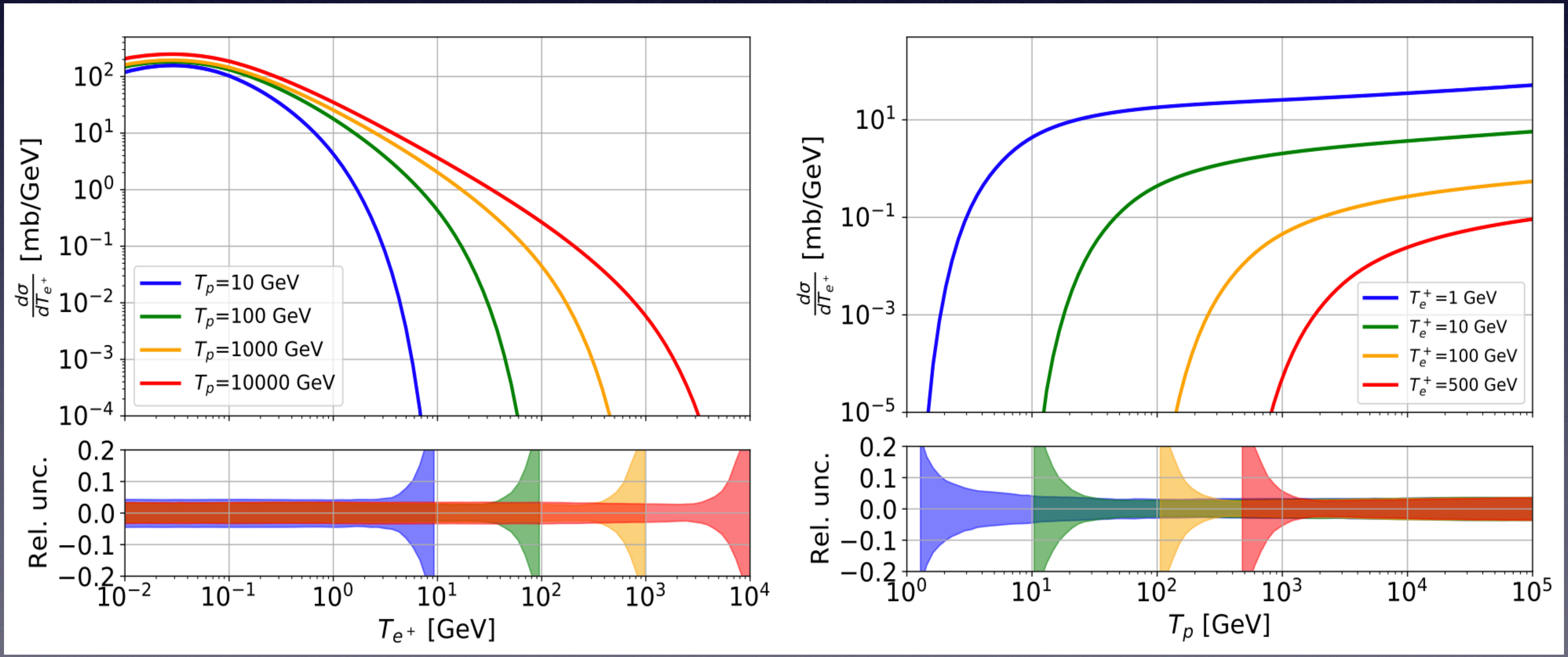

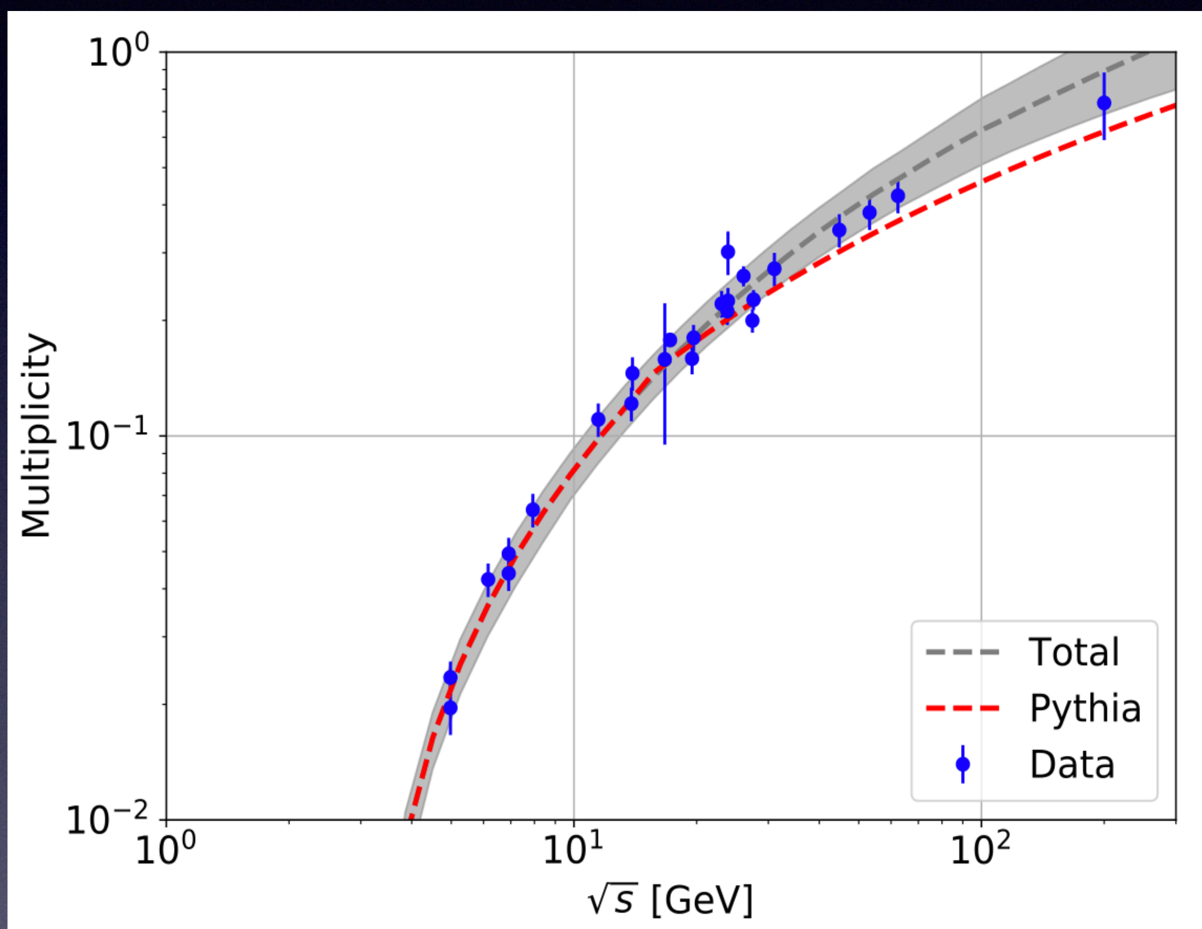
Multiplicity
10^0
10^{-1}
10^{-2}
10^0
10^1
10^2
$\sqrt{s}$ [GeV]
Total
Pythia
Data

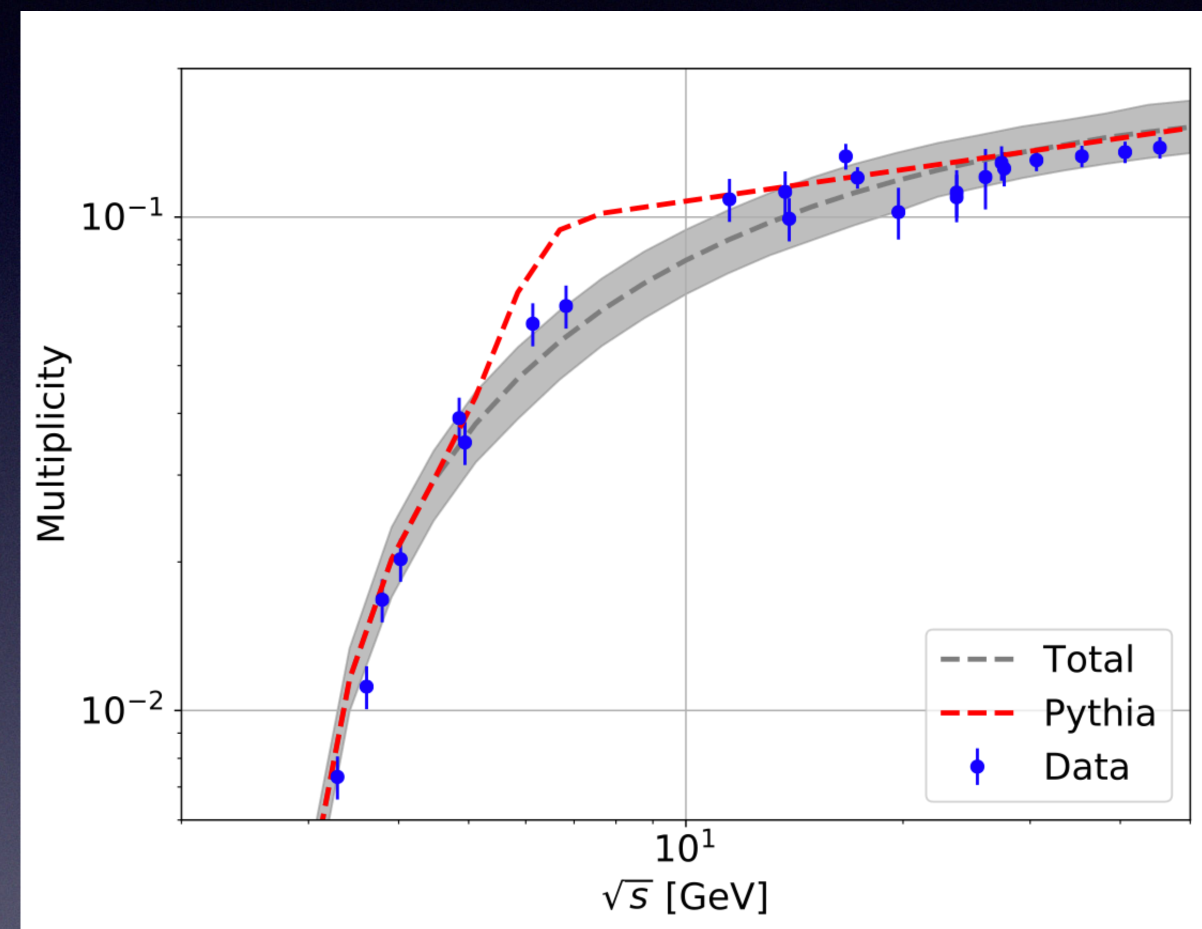
Multiplicity
10^{-1}
10^{-2}
10^1
$\sqrt{s}$ [GeV]
Total
Pythia
Data

Backup

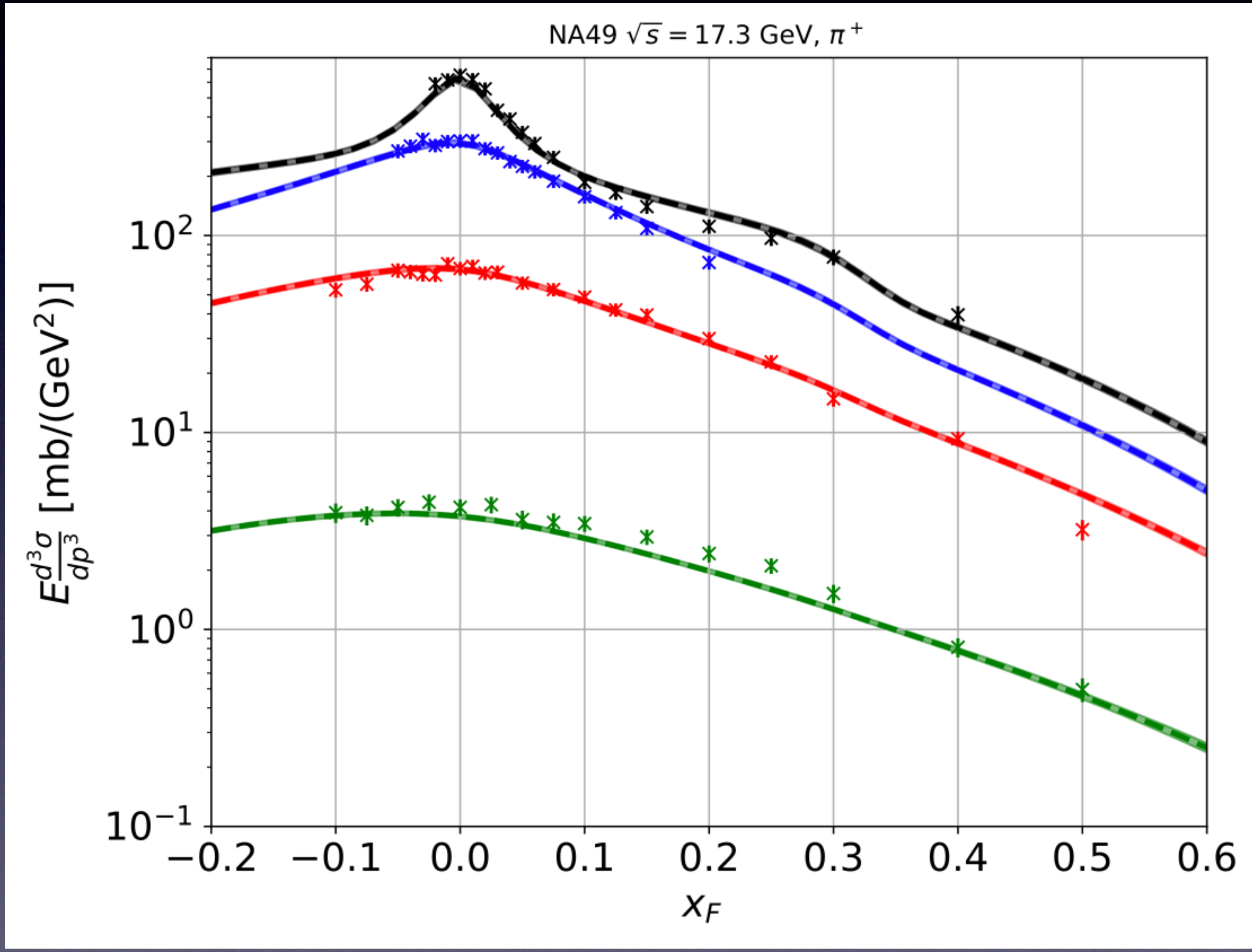

NA49 √s = 17.3 GeV, π⁺
E d³σ/dp³ [mb/(GeV²)]
10²
10¹
10⁰
10⁻¹
−0.2
−0.1
0.0
0.1
0.2
0.3
0.4
0.5
0.6
x_F

Backup

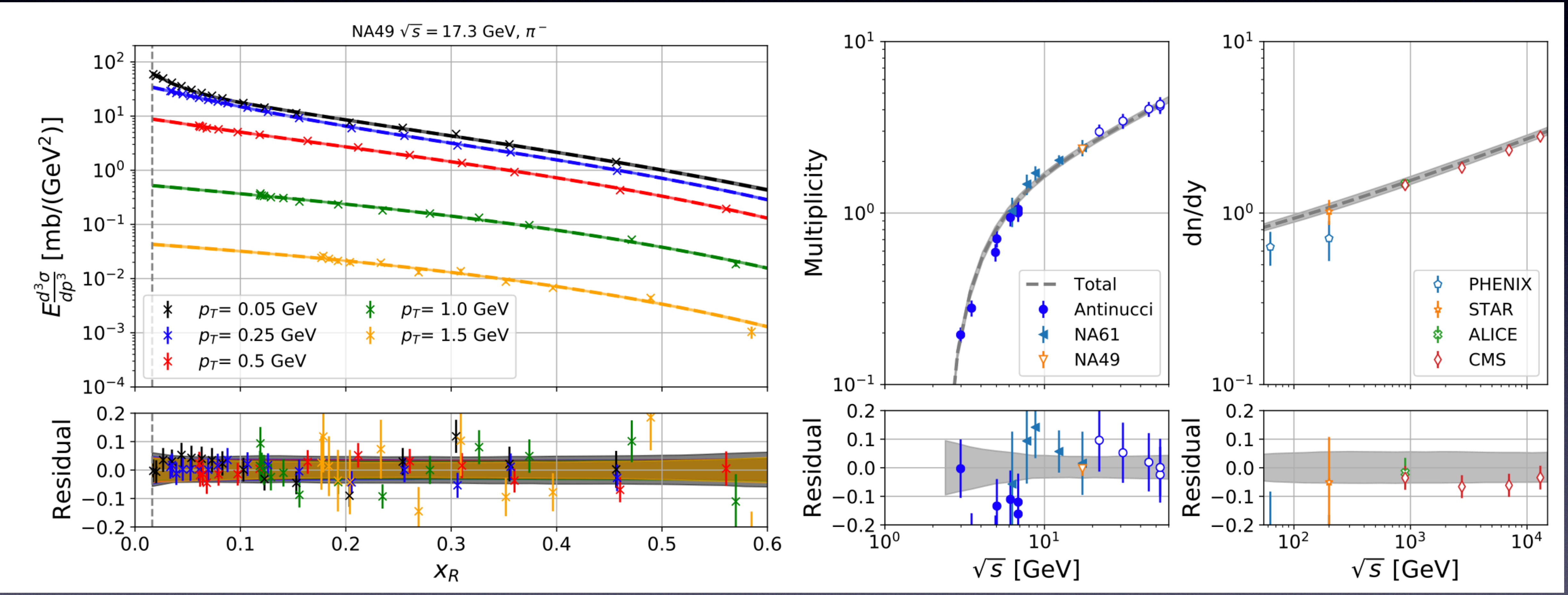
NA49 $\sqrt{s} = 17.3$ GeV, π^-
$E\frac{d^3\sigma}{dp^3}$ [mb/(GeV^2)]
p_T= 0.05 GeV
p_T= 0.25 GeV
p_T= 0.5 GeV
p_T= 1.0 GeV
p_T= 1.5 GeV
Residual
x_R
Multiplicity
Total
Antinucci
NA61
NA49
$\sqrt{s}$ [GeV]
dn/dy
PHENIX
STAR
ALICE
CMS

Backup

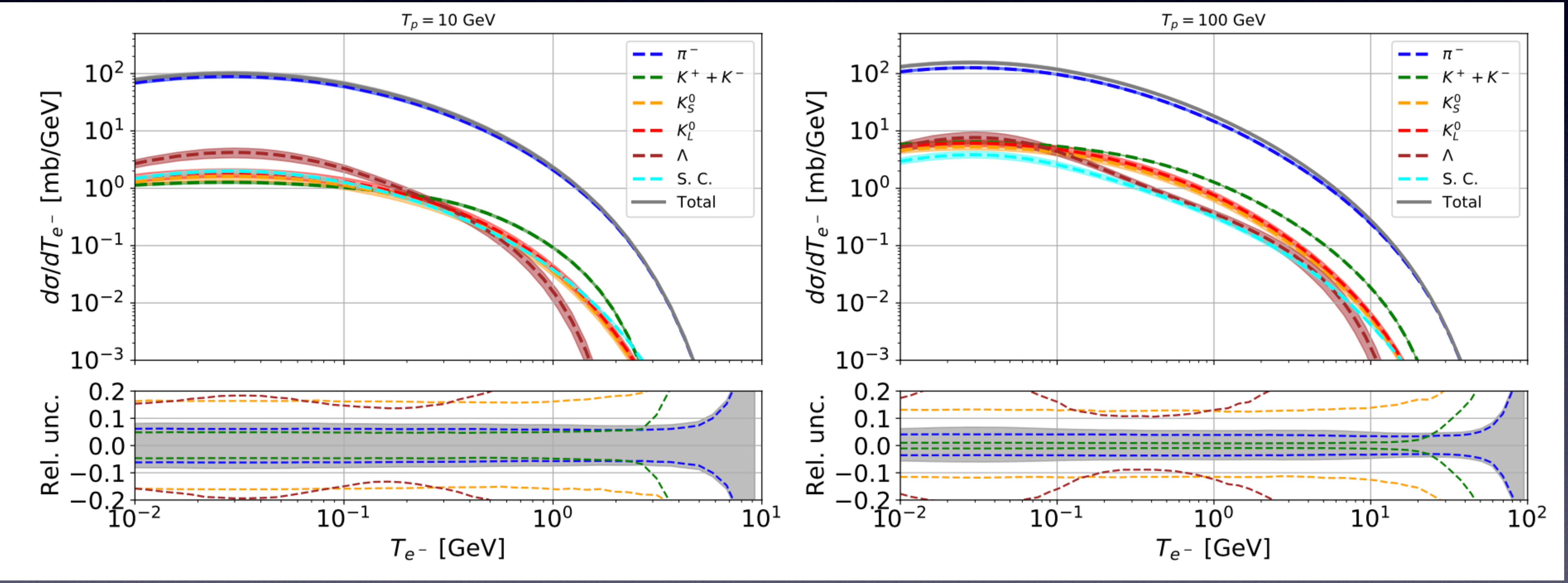

$T_p = 10$ GeV
$T_p = 100$ GeV
$d\sigma/dT_{e^-}$ [mb/GeV]
Rel. unc.
T_{e^-} [GeV]
π^-
$K^+ + K^-$
K_S^0
K_L^0
Λ
S. C.
Total

Backup

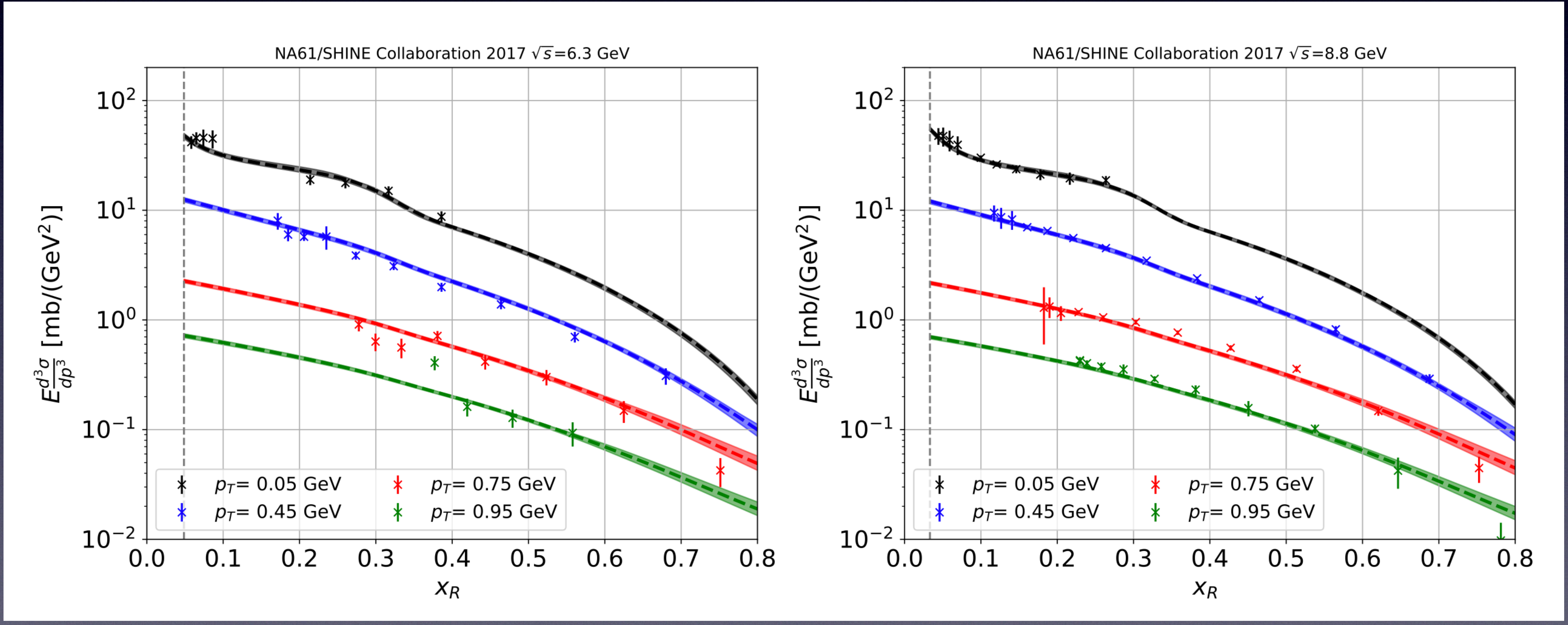

NA61/SHINE Collaboration 2017 √s=6.3 GeV
NA61/SHINE Collaboration 2017 √s=8.8 GeV
$E\frac{d^3\sigma}{dp^3}$ [mb/(GeV^2)]
x_R
p_T= 0.05 GeV
p_T= 0.45 GeV
p_T= 0.75 GeV
p_T= 0.95 GeV

Backup

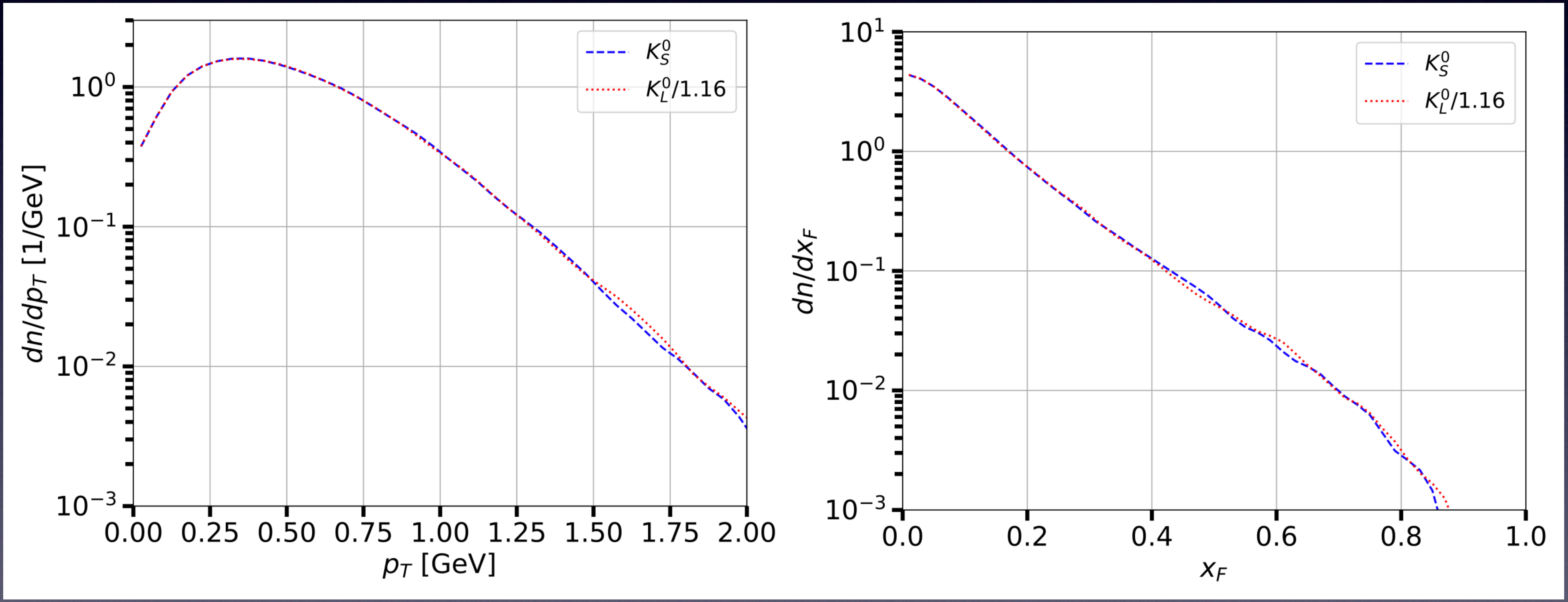

dn/dp_T [1/GeV]
10^0
10^{-1}
10^{-2}
10^{-3}
0.00 0.25 0.50 0.75 1.00 1.25 1.50 1.75 2.00
p_T [GeV]
K_S^0
$K_L^0/1.16$
dn/dx_F
10^1
10^0
10^{-1}
10^{-2}
10^{-3}
0.0 0.2 0.4 0.6 0.8 1.0
x_F
K_S^0
$K_L^0/1.16$

Backup

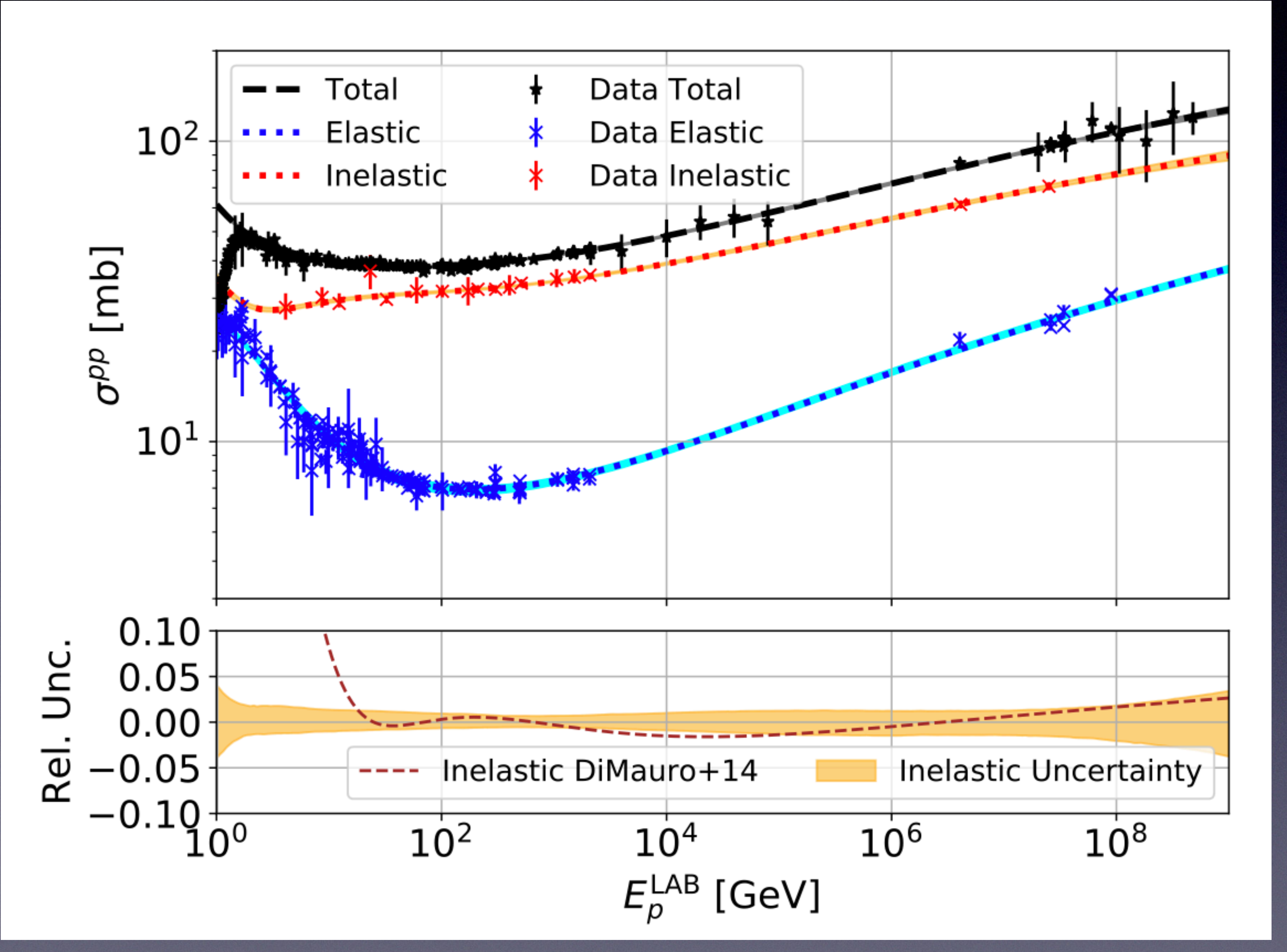

Total
Elastic
Inelastic
Data Total
Data Elastic
Data Inelastic
10^2
10^1
σ^{pp} [mb]
0.10
0.05
0.00
−0.05
−0.10
Rel. Unc.
Inelastic DiMauro+14
Inelastic Uncertainty
10^0
10^2
10^4
10^6
10^8
E_p^{LAB} [GeV]

Backup

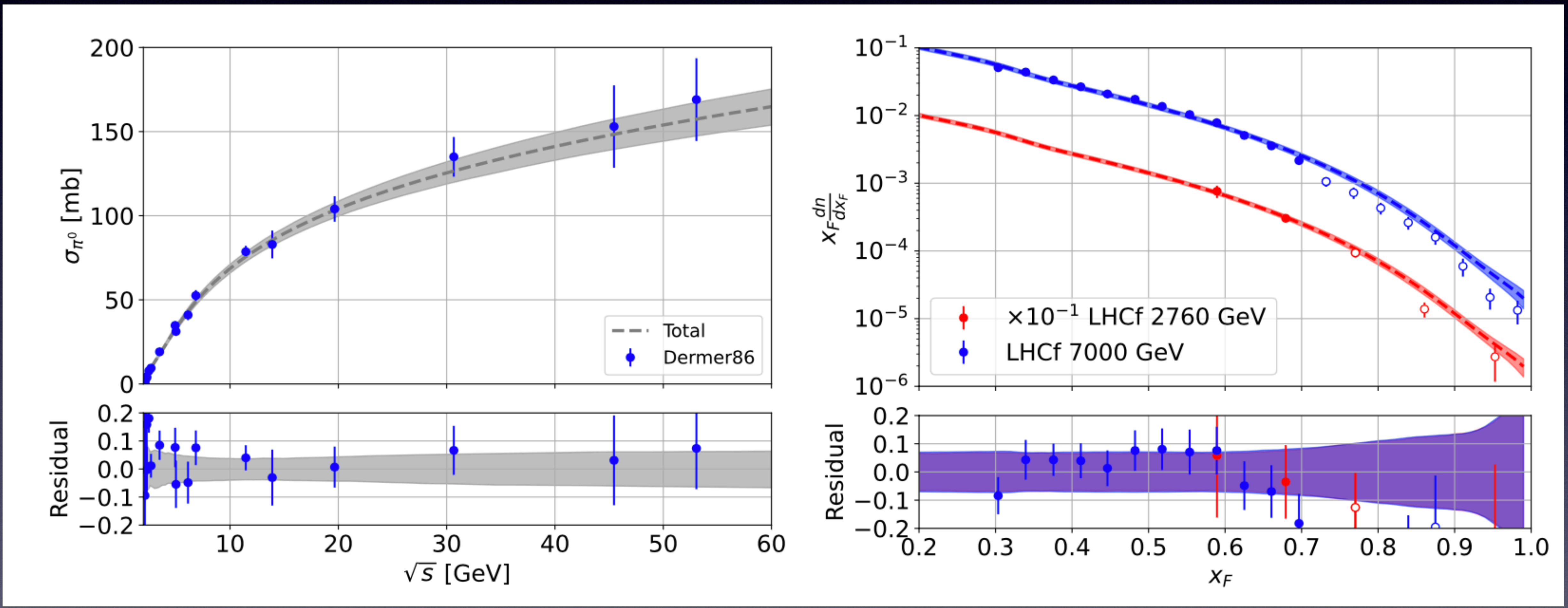

200
150
100
50
0
σ_{π^0} [mb]
Total
Dermer86
0.2
0.1
0.0
−0.1
−0.2
Residual
10
20
30
40
50
60
$\sqrt{s}$ [GeV]
10^{-1}
10^{-2}
10^{-3}
10^{-4}
10^{-5}
10^{-6}
$x_F \frac{dn}{dx_F}$
$\times 10^{-1}$ LHCf 2760 GeV
LHCf 7000 GeV
Residual
0.2
0.3
0.4
0.5
0.6
0.7
0.8
0.9
1.0
x_F

Backup

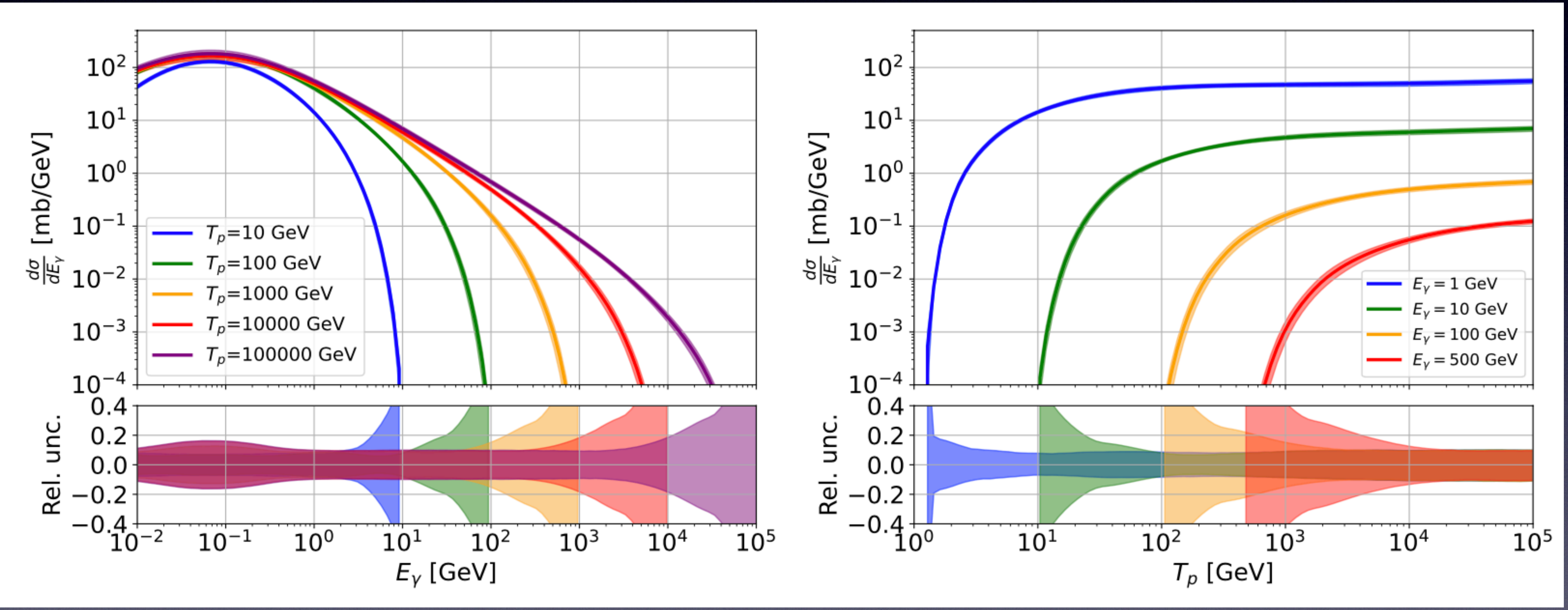

$\frac{d\sigma}{dE_\gamma}$ [mb/GeV]
T_p=10 GeV
T_p=100 GeV
T_p=1000 GeV
T_p=10000 GeV
T_p=100000 GeV
Rel. unc.
E_γ [GeV]
$E_\gamma = 1$ GeV
$E_\gamma = 10$ GeV
$E_\gamma = 100$ GeV
$E_\gamma = 500$ GeV
T_p [GeV]

Backup

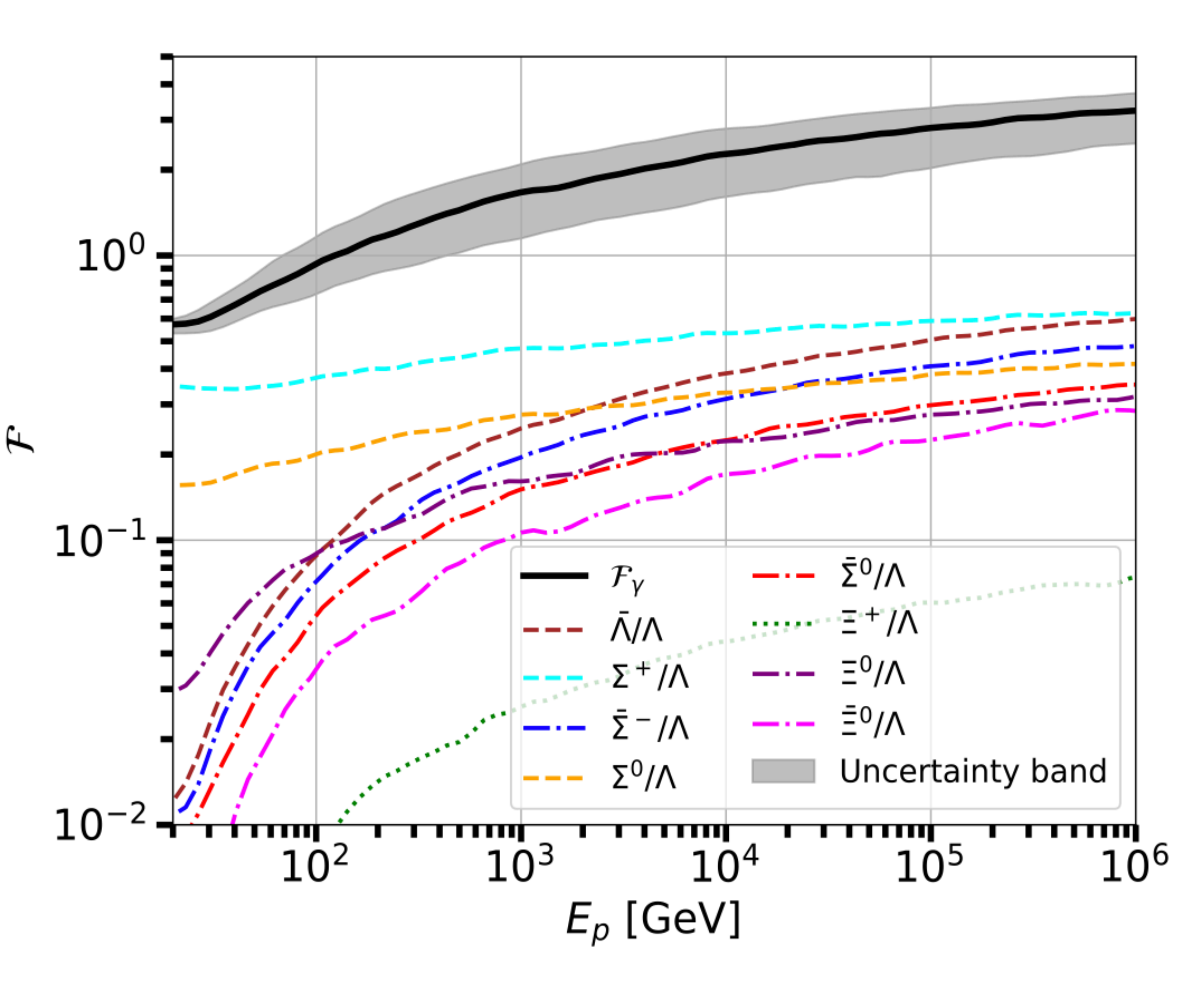

$\mathcal{F}$
E_p [GeV]
10^0
10^{-1}
10^{-2}
10^2
10^3
10^4
10^5
10^6
$\mathcal{F}_\gamma$
$\bar{\Lambda}/\Lambda$
Σ^+/Λ
$\bar{\Sigma}^-/\Lambda$
Σ^0/Λ
$\bar{\Sigma}^0/\Lambda$
Ξ^+/Λ
Ξ^0/Λ
$\bar{\Xi}^0/\Lambda$
Uncertainty band

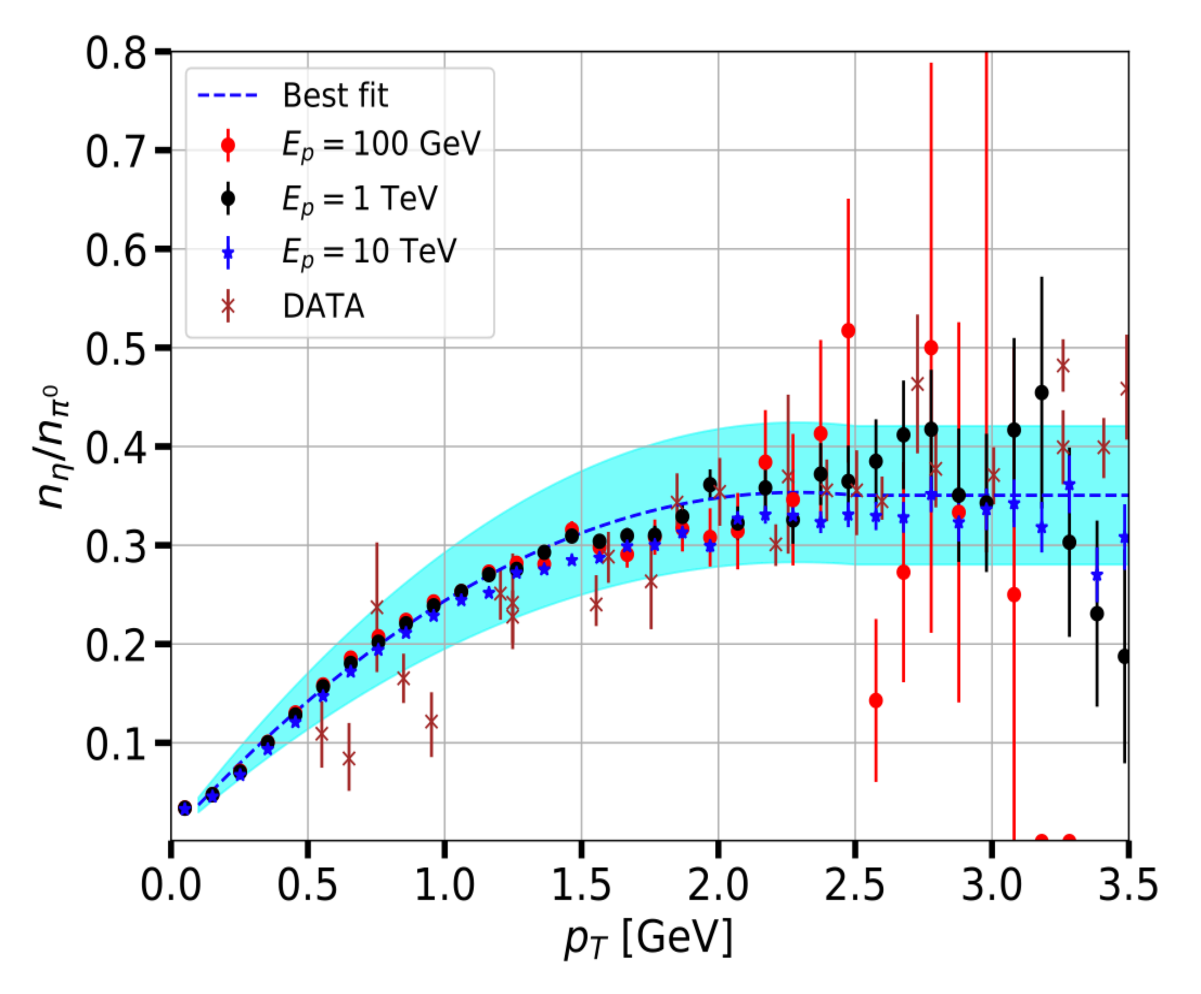

n_η/n_{π^0}
p_T [GeV]
0.8
0.7
0.6
0.5
0.4
0.3
0.2
0.1
0.0
0.5
1.0
1.5
2.0
2.5
3.0
3.5
Best fit
$E_p = 100$ GeV
$E_p = 1$ TeV
$E_p = 10$ TeV
DATA

Backup

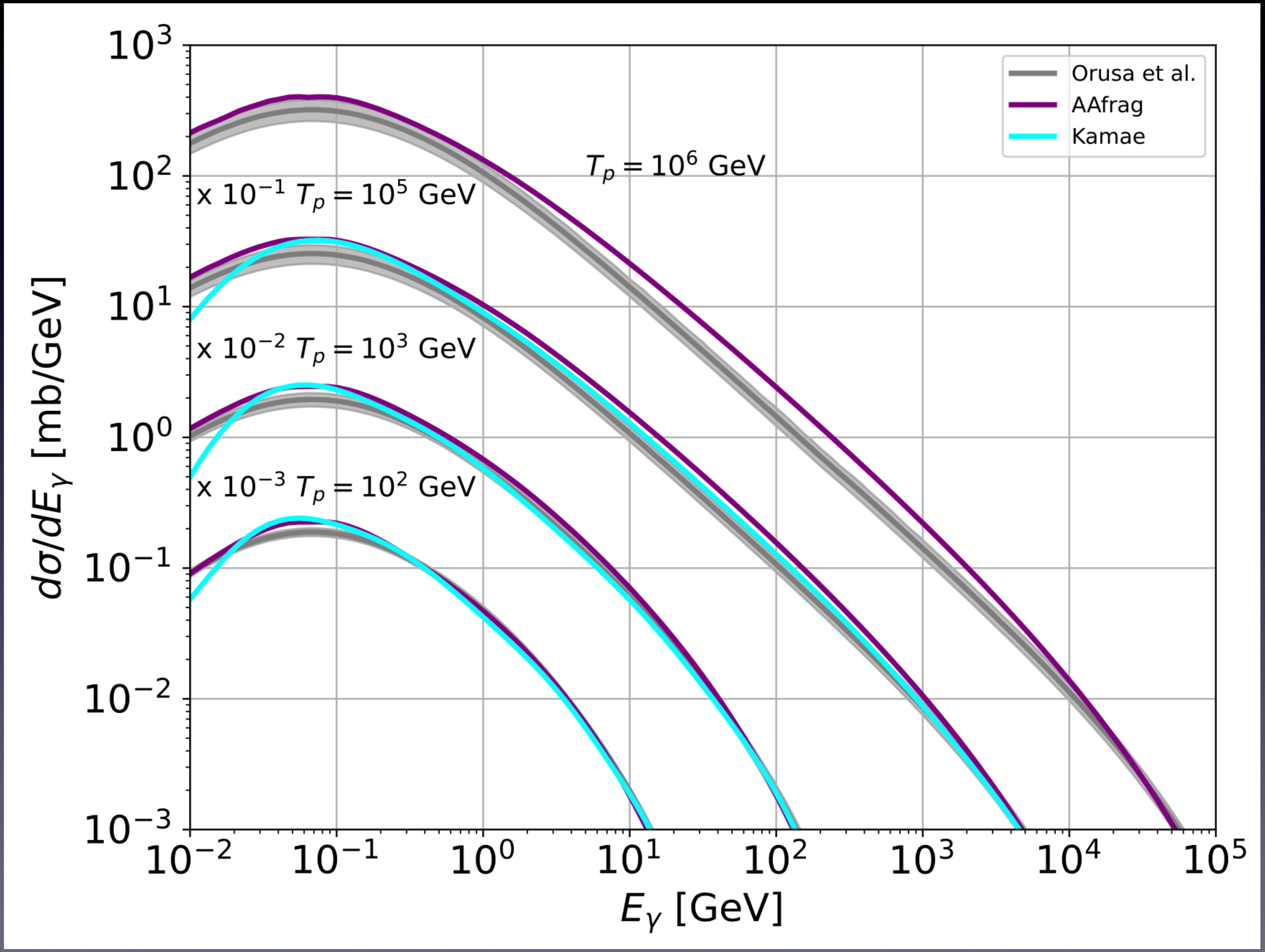

Orusa et al.
AAfrag
Kamae
$T_p = 10^6$ GeV
x 10^{-1} $T_p = 10^5$ GeV
x 10^{-2} $T_p = 10^3$ GeV
x 10^{-3} $T_p = 10^2$ GeV
$d\sigma/dE_\gamma$ [mb/GeV]
E_γ [GeV]
10^3
10^2
10^1
10^0
10^{-1}
10^{-2}
10^{-3}
10^4
10^5